Materials and methods

Materials

Lipofectamine 3000 (L3000008) and BODIPY$^{493/503}$ (D3922) were purchased from Thermo Fisher Scientific. Nile Red (SS1956) was purchased from BIOFUNT. Bovine Serum Albumin (BSA) (B2064), palmitic acid (PA) (P5585), oleic acid (OA) (O1008), puromycin (P7255), compactin (1443216), $^{2}H_2O$ (151882), Oil red O (O0625), and Triton X-100 (T8787) were purchased from Sigma-Aldrich. Simple ChIP Plus Sonication Chromatin IP Kit (56383S) was purchased from Cell Signaling Technology. T0901317 (HY-10626), GW3965 (HY-10627), and CPTH2 (HY-W013274) were purchased from MedChemExpress. Anti-mouse horseradish peroxidase (HRP) (A0216), anti-rabbit horseradish peroxidase (HRP) (A0208), BCA protein concentration assay kit (P0010), MTT (C0009S), reporter gene cell lysis buffer (RG126M), SDS (ST626), SDS-PAGE Sample Loading Buffer (5X) (P0015L) were purchased from Beyotime. Protease inhibitors (04693124001), and Phosphatase inhibitors (4906845001) were purchased from Roche. Nitrocellulose (NC) membrane (HATF00010) was purchased from Millipore. Tris-HCl buffer (T301502) and mevalonate (D304342) were purchased from Aladdin. 4% paraformaldehyde (PFA) (BL539A) was purchased from Biosharp. TG (A110-1-1), TC (A111-1-1), HDL-c (A112-1-1), and LDL-c (A113-1-1) assay kits were purchased from Nanjing Jiancheng Bioengineering Institute. HFD diets (D12492), HFrD diets (D02022704K) and AMLN diets (D09100310) were purchased from Research Diets. FPC diets (TD190142) were purchased from Teklad. HFMRCD diets (XTMRCD-60) and normal diets (1010039) were purchased from Jiangsu Synergetic

Biology Co., Ltd. RNA-easy isolated reagent (R701), HiScript Reverse Transcriptase kit (R123-01), Dual Luciferase Reporter Assay Kit (DL101-01), and qPCR SYBR Green Master Mix (Q111-02) were purchased from Vazyme. Protein A/G agarose bead (sc-2003) was purchased from Santa Cruz Biotech. The mixture of ^{12}C D-glucose and ^{13}C fructose (FRU-011) was purchased from Omicron.

Primary antibodies

Anti-Flag (ab205606), anti-LXRα (ab41902), and anti-SREBP1 (ab3259) antibodies were purchased from Abcam. Anti-GAPDH (AF0006) antibody was purchased from Beyotime. Anti-H3K14ac (7627T), and anti-H3K9ac (9649S) antibodies were purchased from Cell Signaling Technology. Anti-PCAF (A22719), anti-GCN5 (A2224), and anti-Myc (AE010) antibodies were purchased from Abclonal. Anti-p-IκBα (WL02495), anti-IκBα (WL01936), anti-p-p65 (WL02169), anti-p65 (WL01273b), anti-p-SMAD2/3 (WL02305), anti-SMAD2/3 (WL01520), anti-Collagen I (WL0088), and anti-α-SMA (WL02510) antibodies were purchased from Wanleibio. Alexa Fluor® 488 AffiniPure® Alpaca Anti-Rabbit IgG (H+L) (611-545-215) and Alexa Fluor® 594 AffiniPure® Alpaca Anti-Mouse IgG (H+L) (615-585-214) antibodies were purchased from Jackson ImmunoResearch.

Plasmids

pCMV3-C-Flag-p-SREBP1c, pCMV3-C-Flag-m-SREBP1c, pCMV3-C-HA-RXRα, pCMV3-C-Flag-GCN5, pCMV3-C-Myc-GCN5, pCMV3-C-Flag-GCN5 (E575Q), pCMV3-C-Myc-LXRα, pCMV3-C-Myc-LXRα (1-163 aa), pCMV3-C-Myc-LXRα (164-326 aa), pCMV3-C-Myc-LXRα (327-447 aa), pCMV3-C-Flag-GCN5 (1-407 aa),

pCMV3-C-Flag-GCN5 (408-656 aa), pCMV3-C-Flag-GCN5 (657-837 aa) plasmids were constructed by gene synthesis and site-directed mutagenesis.

Cell culture

The HEK293T (293T cells), RAW264.7, and HepG2 cell lines were acquired from the American Type Culture Collection (ATCC). The HL-7702 cells were procured from Keygen Biotechnology. All cell lines were cultured at 37 °C with 5% CO_2 in the indicated medium.

Culture medium

Medium A was prepared using DMEM (Keygen, KGL1206) supplemented with 10% fetal bovine serum (Gibco, A5670701), 100 units/ml penicillin, and 100 μg/ml streptomycin sulfate. Medium B consisted of an equal-volume mixture of Ham's F-12K (Gibco, 21127030) and DMEM, supplemented with 5% LPDS (Kalen Biomedical, 880100), 10 μM compactin (Sigma-Aldrich, 1443216), and 50 μM mevalonate (Aladdin, D304342).

Mouse primary hepatocyte isolation

Animals were first anesthetized using isoflurane (1.5% in O_2). A catheter was then inserted into the vena cava, and the portal vein was cut. The liver was subsequently perfused via the catheter with oxygenated, 37°C Buffer A (1× PBS, 5 mM EGTA). This was followed by perfusion with oxygenated, 37°C Buffer B (1× PBS, 1 mM $CaCl_2$, collagenase type IV). Finally, the liver was transferred to a Petri dish containing Buffer C (1× PBS, 2 mM $CaCl_2$, 0.6% BSA) and gently dissociated using forceps. Liver perfusions were centrifuged at 48 g for 5 minutes after digestion using sterile gauze.

Next, primary hepatocytes were isolated from mice using sterile gauze. A pellet of hepatocytes was resuspended in Medium B, and the supernatant was discarded after three washes. In collagen-coated plates, hepatocytes were plated, and cell viability was confirmed via the trypan blue exclusion test. Cell viability greater than 70% was considered acceptable for moving forward with the research.

Prediction of transcription factors binding to the KAT2A promoter

Using the JASPAR (jaspar.genereg.net) tool to scan transcription factors on the 2000+200bp region of the KAT2A promoter, under the screening condition of p value $< 10^{-5}$, search for transcription factors targeting the motif sequences on the human and mouse promoter regions. The intersection of the two is taken to screen out possible transcription factors, and there are 6 of them. After analyzing the existing literature on these 6 transcription factors, 4 related to lipid metabolism were selected for further study.

Viability assay

Cell viability was assessed in HepG2, HL-7702, and primary hepatocytes using the MTT assay. Briefly, cells were plated in 96-well plates at a density of 1×10^4 cells per well. After 24 hours, the cells were treated with the specified concentrations of CPTH2 for another 24 hours. Then, 10 μl of MTT solution (5 mg/ml) was added to each well, and the plates were incubated at 37 °C for 4 hours. Subsequently, 100 μl of formazan solution was added to each well, followed by incubation at 37 °C for 3–4 hours. Absorbance was measured at 570 nm using a microplate reader (BMG POLARstar Omega).

BODIPY$^{493/503}$ and Nile Red staining

Cells were fixed with 4% paraformaldehyde and then stained with 1 μM Nile Red or 5 μM BODIPY$^{493/503}$ for 30 min at room temperature in the dark. After being stained with DAPI, excess dye was washed away with PBS three times. The fluorescence of intracellular lipid droplets was photographed by a laser confocal microscope (Olympus FV3000). ImageJ (Version 1.5a) was used to quantify intracellular neutral lipids.

Western blotting

After collection, cells were solubilized in lysis buffer supplemented with SDS, loading buffer, protease inhibitors, and phosphatase inhibitors. Samples were then thermally denatured at 95 °C for 10 minutes and subjected to electrophoretic separation on 8–12% SDS-polyacrylamide gels. Subsequently, proteins were transferred onto nitrocellulose membranes via electroblotting. Membranes were blocked for 1 hour at room temperature with 5% non-fat dry milk and then incubated with primary antibodies at 4 °C overnight. Following thorough washing, membranes were exposed to HRP-conjugated secondary antibodies for 1 hour at room temperature. Detection was carried out using an enhanced chemiluminescence substrate, and blot images were captured with a Tanon 5200 imaging system (Tanon, China). Quantitative analysis of band intensity was conducted using ImageJ software (Version 1.5a).

Cellular, liver, and serum lipid determination

A subset of cells was reserved for protein quantification via BCA assay, while the remainder underwent lipid extraction. Cellular total cholesterol (TC) and triacylglycerol (TG) were extracted in chloroform/methanol (2:1, v/v) at room

111 temperature for 3 h. After adding 500 μl of 0.1 M NaCl, samples were vortexed,
112 centrifuged, and the lower organic phase collected and dried under nitrogen. Dried
113 lipids were redissolved in 50 μl ethanol with 1% Triton X-100 (Sigma-Aldrich, T9284).
114 TG and TC levels were determined using commercial assay kits and normalized to
115 protein content.
116 For hepatic TG and TC measurement, 50 mg liver tissue was homogenized in PBS. Part
117 of the homogenate was used for BCA protein assay; 0.4 ml was mixed with 1.6 ml
118 chloroform/methanol for extraction as above.
119 Serum TG, TC, HDL-c, and LDL-c were measured using corresponding kits per
120 manufacturer's protocols.
121 **Measurement of *de novo* fatty acid synthesis**
122 *KAT2A* knockout and wild-type HL-7702 cells were treated under specified conditions
123 in Medium B for 16 h. The *de novo* fatty acid synthesis rate was assessed by incubation
124 with a 12 μCi/ 60 mm dish of [^{14}C] acetate for 2 h. After washing, cells were lysed in
125 0.1 N NaOH and saponified by autoclaving. Nonpolar lipids (cholesterol) were
126 extracted using petroleum ether and evaporated under nitrogen. Following acidification
127 with concentrated HCl, polar lipids (fatty acids) were similarly extracted, dried, and
128 dissolved in 5 ml scintillation cocktail for DPM measurement.
129 **Oxygen consumption rate (OCR)**
130 HL-7702 cells were plated in Seahorse XF96 microplates (Agilent Technologies, USA)
131 at 5×10^4 cells/well and treated with OA (200 mM) and PA (100 mM). Prior to OCR
132 assessment, cells were incubated for 1 hour at 37 °C in a CO_2-free incubator using XF

base minimal DMEM supplemented with 10 mM glucose, 0.5 mM L-carnitine, and 1 mM L-glutamine. OCR was monitored using the Seahorse XFe96 extracellular flux assay kit under calibrant conditions. Sequential injections of 2 μM etomoxir, 2.5 μM oligomycin, 1 μM FCCP, and 0.5 μM rotenone/antimycin A were performed during the assay. Additionally, 30 μl of BSA-control or BSA-palmitic acid (BSA-PA) was introduced into each well before measurement. Data were acquired on a Seahorse XFe96 Analyzer and analyzed with Wave 2.6.1 software.

FFA uptake

The uptake of free fatty acids (FFA) was quantified utilizing a fluorometric assay kit (Abcam, ab176768). HL-7702 cells were seeded at 1×10^5 cells per well, resuspended in PBS, and maintained at 37 °C in a CO_2 incubator for 30 minutes. Subsequently, a fluorescent FFA probe was added. Following an additional incubation period of 1 hour, fluorescence intensity was detected in bottom-read mode with excitation/emission set at 485/515 nm (or FITC channel) on a microplate reader.

Cholesterol efflux test

RAW264.7 cells were inoculated at a density of about 1×10^6 cells/well in a 6-well plate. The next day, the medium was removed and treated for 24 hours with drugs or other means. Then, 1.5 μM 22-NBD cholesterol was added to a medium containing 2.5% FBS for 1 h. The cells were washed twice with Puck buffer and placed in a serum-free medium. Efflux was initiated by adding HDL (10 μg/ml). Following 4 hours of incubation, cells were harvested and resuspended in FACS buffer. Fluorescence (FL-1) was quantified via flow cytometry, and data were analyzed using Cell Quest Pro

software. HDL-dependent cholesterol efflux was calculated as: (fluorescence without HDL − fluorescence with HDL) / fluorescence without HDL × 100%.

Reporter gene assay

Promoter-reporter constructs (SREBP-1c-Luc, SREBP-1c mtLXRE-Luc, ABCA1-Luc, and ABCA1 mtLXRE-Luc) were generated by PCR-based cloning, with primer sequences provided in Table 1. HL-7702 cells were seeded in 96-well plates, transfected with the corresponding luciferase reporter plasmids, and treated as indicated. After treatment, cells were lysed using reporter gene lysis buffer (Beyotime, RG0036) for 30 minutes at room temperature. Lysates from each well were transferred to a white 96-well plate. Protected from light, luciferase substrate (Vazyme, DL101-01) was added, and luminescence was immediately measured using a BMG POLARstar Omega microplate reader. Luminescence values were normalized to the protein concentration of each sample.

Table 1. List of primers used for cloning.

Cloning Oligo Name	Sequence (5'→3')[A]
SREBF1c (-550/+42) For	CGGGGTACCCCCCCCTCCTTGAAACAA
SREBF1c (-550/+42) Rev	CCGCTCGAGCCTAGGGCGTGCAGACGC
SREBF1c (mt LXRE a) For	ACGACAGAGTCCGCCAGAATCCCCAGC
SREBF1c (mt LXRE a) Rev	GCTGGGGATTCTGGCGGACTCTGTCGT
SREBF1c (mt LXRE b) For	AAGGCGGAAGTCCGCTAGAATCCCCGGC
SREBF1c (mt LXRE b) Rev	GCCGGGGATTCTAGCGGACTTCCGCCTT
ABCA1 (-928/+101) For	CGGGGTACCTAAGTTGGAGGTCTGGAG
ABCA1 (-928/+101) Rev	CCGCTCGAGGCTCTGTTGGTGCGCG
ABCA1 (mt LXRE) For	AGGCTTTGTGTGATAGTAACTGCTGCGCT
ABCA1 (mt LXRE) Rev	AGCGCAGCAGTTACTATCACACAAAGCCT

[A] Mutated nucleotides are underlined.

Structure prediction

The amino acid sequences for human GCN5 and LXRα were retrieved from the UniProt, with the respective Protein IDs: GCN5 (Q92830, https://www.uniprot.org/uniprotkb/Q92830/entry), LXRα (Q13133, https://www.uniprot.org/uniprotkb/Q13133/entry). 3D complex structures of GCN5 and LXRα were predicted using AlphaFold3 (https://www.alphafoldserver.com). Resulting models were visualized and analyzed with PyMOL.

qRT-PCR

Total RNAs were extracted by RNA-easy isolated reagents. cDNA was reverse transcribed with the HiScript Reverse Transcriptase kit. qRT-PCR was carried out on a LightCycler 96 system (Roche) with SYBR Green Master Mix. The relative expression of genes was calculated by △△CT method. Primer sequences are provided in Table 2.

Table 2. Primers for RT-qPCR

Gene	Forward	Reverse
Mus musculus		
Kat2a	AATTCTCCCATCTGGGAGTCAGG	ATGGAAGGACTGAAGCTGGGTAC
Kat2b	CCGTGTCATTGGTGGTATCTGTT	AGGAAGTTGAGGATCTCGTGCTT
β-actin	GGCTGTATTCCCCTCCATCG	CCAGTTGGTAACAATGCCATG
Srebf1	GGAGCCATGGATTGCACATT	GGCCCGGGAAGTCACTGT
β-actin	GGCTGTATTCCCCTCCATCG	CCAGTTGGTAACAATGCCATG
Acc	GCCCCATATGATCCTCGGTG	ATTCCCCCTAACCTGGCTCT
Fasn	CTGACTCGGCTACTGACACG	AATGGGGTGCACAAGGAACA
Scd1	GGGTGCCGTGGGCGA	GGAACTCAGAAGCCCAAAGC
Scd2	GCATTTGGGAGCCTTGTACG	AGCCGTGCCTTGTATGTTCTG
Fads2	GGCCACTTAAAGGGTGCCTC	GGCTCTTTATGTCCGGGTCC
Acly	CAGCCAAGGCAATTTCAGAGC	CTCGACGTTTGATTAACTGGTCT
Srebf2	GCGTTCTGGAGACCATGGA	ACAAAGTTGCTCTGAAAACAAATCA
Pcsk9	GAGACCCAGAGGCTACAGATT	AATGTACTCCACATGGGGCAA
Fatp1	CGCTTTCTGCGTATCGTCTG	GATGCACGGGATCGTGTCT
Ldlr	TGACTCAGACGAACAAGGCTG	ATCTAGGCAATCTCGGTCTCC
Cd36	ATGGGCTGTGATCGGAACTG	GTCTTCCCAATAAGCATGTCTCC
Apob	AAGCACCTCCGAAAGTACGTG	CTCCAGCTCTACCTTACAGTTGA
Apoe	CTGACAGGATGCCTAGCCG	CGCAGGTAATCCCAGAAGC
Fatp4	TGTGGTGCACAGCAGGTATT	AGTCATGCCGTGGAGTAAGC
Plin2	GACCTTGTGTCCTCCGCTTAT	CAACCGCAATTTGTGGCTC

Mttp	CTCTTGGCAGTGCTTTTTCTCT	GAGCTTGTATAGCCGCTCATT
Pparα	AGAGCCCCATCTGTCCTCTC	ACTGGTAGTCTGCAAAACCAAA
Acsl1	TGCCAGAGCTGATTGACATT	GGCATACCAGAAGGTGGTGAG
Acadm	AGGGTTTAGTTTTGAGTTGACGG	CCCCGCTTTTGTCATATTCCG
Cpt1a	CTCCGCCTGAGCCATGAAG	CACCAGTGATGATGCCATTCT
Cpt1b	GCACACCAGGCAGTAGCTTT	CAGGAGTTGATTCCAGACAGGTA
Cpt1c	TCTTCACTGAGTTCCGATGGG	ACGCCAGAGATGCCTTTTCC
Gpat	ACAGTTGGCACAATAGACGTTT	CCTTCCATTTCAGTGTTGCAGA
Ucp2	ATGGTTGGTTTCAAGGCCACA	CGGTATCCAGAGGGAAAGTGAT
Acox1	TCCAGACTTCCAACATGAGGA	CTGGGCGTAGGTGCCAATTA
Me	GGACTTCTATGACCTGTACGGA	GCTGCGTGTAATACTCGACCA
Pdk4	AGGGAGGTCGAGCTGTTCTC	GGAGTGTTCACTAAGCGGTCA
Abca1	CGTTTCCGGGAAGTGTCCTA	GCTAGAGATGACAAGGAGGATGGA
Abcg5	TGGATCCAACACCTCTATGCTAAA	GGCAGGTTTTCTCGATGAACTG
Abcg8	ACGTATGTACGTGGGGTGTC	GGGTTCATCCAGAATGAGGA
Il6	TAGTCCTTCCTACCCCAATTTCC	TTGGTCCTTAGCCACTCCTTC
Il1b	CCGTGGACCTTCCAGGATGA	GGGAACGTCACACACCAGCA
Cxcl1	GCTGGGATTCACCTCAAGAA	TTGGGGACACCTTTTAGCAT
Cxcl15	GGCCCAATTACTAACAGGTTCC	GTCTCCCGAATTGGAAAGGGA
Cxcl10	ATGACGGGCCAGTGAGAATG	ATGATCTCAACACGTGGGCA
Acta2	GTCCCAGACATCAGGGAGTAA	TCGGATACTTCAGCGTCAGGA
α-Sma	CCCAGACATCAGGGAGTAATGG	TCTATCGGATACTTCAGCGTCA
Col1a1	TGCTAACGTGGTTCGTGACCGT	ACATCTTGAGGTCGCGGCATGT
Ctgf	TGACCCCTGCGACCCACA	TACACCGACCCACCGAAGACACAG
Tgfβ	ATTTGGAGCCTGGACACACA	GAGCGCACAATCATGTTGGA
Col3a1	ACGTAAGCACTGGTGGACAG	CCGGCTGGAAAGAAGTCTGA
Homo sapiens		
SREBF1	ACAGTGACTTCCCTGGCCTAT	GCATGGACGGGTACATCTTCAA
ACC	ATGTCTGGCTTGCACCTAGTA	CCCCAAAGCGAGTAACAAATTCT
FASN	CCGAGACACTCGTGGGCTA	CTTCAGCAGGACATTGATGCC
FADS2	GACCACGGCAAGAACTCAAAG	GAGGGTAGGAATCCAGCCATT
SCD1	TCTAGCTCCTATACCACCACCA	TCGTCTCCAACTTATCTCCTCC
SCD2	CTCTGCGAGTGAATTTGGC	GATCATCGGCTTGGTTGC
GAPDH	GCACCGTCAAGGCTGAGAAC	TGGTGAAGACGCCAGTGGA
KAT2A	CAGGGCTTCACGGAGATTGT	CTTGGGCACCTTGATGTCCT
KAT2B	CTGGAGGCACCATCTCAACGAA	ACAGTGAAGACCGAGCGAAGCA
GAPDH	GCACCGTCAAGGCTGAGAAC	TGGTGAAGACGCCAGTGGA
ABCA1	TGCTAATTGCCAGACGGAG	GGGTACTTGCCAAAGGGTG
ABCG5	CTGAGGTTGCCCGATTTG	ATTTGGATTTTGGACGATA
ABCG8	TTTCCAACGACTTCCGAGAC	GCCTCAGCGATTCCTTGATTAT

Knockout of *KAT2A* by CRISPR-Cas9

A CRISPR-Cas9 genome editing system was applied to establish the *KAT2A* KO cell. Briefly, sgRNA sequence (5'-ATGGGGCAAACTCTCCAATC-3') was designed with the Broad Institute CRISPick tool

(https://portals.broadinstitute.org/gppx/crispick/public) and cloned into pUC-CBh-gRNA vector named pUC-CBh-*KAT2A*-gRNA. HL-7702 cells were transfected with the donor construct EF1A-GFP-T2A-Puro (conferring puromycin resistance) using Lipofectamine 3000. After 48 hours, transfected cells were selected with puromycin (2 μg/ml) for 72 h. Single colonies were isolated, and *KAT2A* knockout was confirmed by western blot.

Chromatin immunoprecipitation (ChIP) and ChIP-seq analysis

The ChIP assay was carried out using the Simple ChIP® Plus Sonication Chromatin IP Kit (Cell Signaling Technology, 56383S). Following treatment, cells were cross-linked with 1% formaldehyde for 10 min at room temperature and quenched with 0.125 M glycine for 5 min. For liver tissues, approximately 100 mg was minced into 1 mm^3 pieces and incubated in PBS containing protease inhibitors before fixation. Cells were washed twice with cold PBS, collected in PBS with protease inhibitors, and centrifuged at 1000 g for 5 min at 4 °C. The pellet was resuspended in Cell Lysis Buffer and lysed on ice for 10 min twice. Nuclei were lysed with Nuclear Lysis Buffer, and chromatin was sheared using a Branson SFX250 Sonifier (50% amplitude, 6 min cycle, 1 s on/off). After centrifugation at 21,000 g for 10 min at 4 °C, the supernatant was collected. Each 10 μg of chromatin was immunoprecipitated with 2 μg of specific antibody or control IgG overnight at 4 °C, followed by incubation with Protein G beads for 2 h at 4 °C. Beads were washed, and chromatin was eluted and reverse cross-linked. DNA was purified and quantified by qPCR. Primer sequences are listed in Table 3.

Table 3. Primers for ChIP-qPCR

Gene	Forward	Reverse
Homo sapiens		
SREBF1c (LXRE)	GAGAACCCGACACGAGGC	TTGCGAGGTTACTCACGGTC
ABCA1 (LXRE)	ATCCCTACCCTTGTGAGCCT	CGAGGTCACTCACTTGGCTT
SREBF1c (Non-LXRE)	TGTGACTGGCTCACCGTAGA	CTGTCCATAGATGGCCCTGG
ABCA1 (Non-LXRE)	TGTCATTGGTTCCCTGGGTG	CGGGGACCTTACCTGGAAAC
Mus musculus		
SREBF1c (LXRE)	AGGCTCTTTTCGGGGATGG	TGGGGTTACTGGCGGTCAC
ABCA1 (LXRE)	GGGGAAAGAGGGAGAGAACAG	GAATTACTGGTTTTTGCCGC
SREBF1c (Non-LXRE)	TTTGTCATTGGCTGTGGTCTTC	CGGCATGGTCCTGATTGC
ABCA1 (Non-LXRE)	GGCAGTGCCTTTGTAGCCTATG	GGTTCCACACCAGAGTTTCACA

ChIP-seq data were obtained from the GEO database (GCN5 ChIP-seq: GSM1003804 and GSE94229; H3K9ac ChIP-seq: GSM1000141 and GSM918712). Raw sequencing reads were trimmed to remove adapter sequences and low-quality fragments using Skewer (v0.2.2). Quality control was performed with FastQC (v0.11.5). Cleaned reads were aligned with the mm9 mouse genome by Bowtie2 (version 2.5.2). Peak calling for tissues was performed using MACS2 (version 2.1.1) to obtain protein and DNA interaction binding sites. ChIP-seq peaks were visualized with IGV (version 2.17.2). Heatmaps were created using R 3.6.1 and the pheatmap package (1.0.12).

RNA-seq analysis

KAT2A knockout and wild-type HL-7702 cells were separately seeded into 6-well plates and treated with PAOA for 24 h, and livers of *Kat2a*^{HKO} mice and *Kat2a*^{flf} mice which fed with 10 weeks HFD diet, then total RNA was extracted using RNA-easy isolated reagent. RNA quantification was detected using NanoPhotometer (Thermo Fisher), followed by examination of RNA integrity and concentration with Agilent 2100 RNA Nano 6000 Assay Kit (Agilent Technologies). mRNA was enriched with Oligo d(T) Magnetic Beads, fragmented, and converted into double-stranded cDNA. The cDNA underwent end repair, adenylation, adapter ligation, and size selection (~350 bp).

After PCR amplification, the resulting library was quantified with Qubit 3.0 (Thermo Fisher) and quality-checked using the Agilent 2100 Bioanalyzer (Agilent Technologies). Sequencing was performed on an MGI DNBSEQ-T7 platform. Raw reads were processed with Fqtools Plus to remove adapters and low-quality sequences. Clean reads were aligned to the hg38 reference genome using HISAT2 (v2.2.1). Differential gene expression analysis was conducted with DESeq2 (v23.1.0) under thresholds of $|\log_2 FC| \geq 1$ and p-value ≤ 0.05. Gene Ontology enrichment was performed using cluster Profiler (v3.5.1; p-value < 0.05). Visualization was carried out with GraphPad Prism (v8), including heatmaps and volcano plots.

Metabolomics

Sample extraction.

Liver tissues from *Kat2a*^{HKO} mice and *Kat2a*$^{fl/fl}$ mice were snap-frozen, pulverized, and aliquoted. Metabolites were extracted using a two-phase system. Powdered tissue was homogenized in 50% methanol and acetonitrile. Phase separation was induced by adding methylene chloride and water, followed by vortexing and centrifugation (4℃, 20 min). The lower organic phase was collected and dried under N_2 for LC-MS analysis of fatty acids. The upper aqueous phase was processed for two analyses: one aliquot was dried, reconstituted in water, and analyzed by LC-MS for CoA species; the remainder was dried, derivatized, and subjected to GC-MS for polar metabolites (DHAP, Glycerol, Glycerol-3P, and Citric acid).

Free and esterified fatty acids analysis by LC-MS

The dried organic phase was reconstituted in a methanolic KOH solution containing an

internal standard (rD27-myristic acid) for saponification. After vortexing, sonication, and incubation, methylene chloride was added, and the mixture was recentrifuged. The aqueous layer was acidified, and free fatty acids were extracted with hexane. The organic layer was dried, reconstituted in methyl acetate, and derivatized with tetramethylammonium hydroxide to generate fatty acid methyl esters (FAMEs). Chromatographic separation was carried out using an Acquity UPLC BEH C18 column (2.1 × 100 mm, 1.7 μm) maintained at 55°C with a flow rate of 0.3 ml/min. Mobile phase A consisted of water-acetonitrile (40:60, v/v) and mobile phase B was isopropanol-acetonitrile (90:10, v/v), both containing 5 mM ammonium formate and 0.1% formic acid. A 35-min gradient was used. Mass spectrometry was conducted on a SCIEX X500B QTOF instrument using both positive and negative ESI modes. Data were acquired in data-independent mode over m/z 100–1250. Quality control samples were analyzed throughout the sequence to ensure instrument stability. Signal intensities were normalized to protein concentration, and data were processed using SCIEX OS software (v. 3.0).

Acyl-CoA analysis by LC-MS/MS

Acyl-CoA species were quantified using HILIC-MS/MS with an Agilent 6470 QQQ mass spectrometer. Chromatographic separation was achieved on a Waters XBridge BEH Amide column (2.1 × 150 mm, 2.5 μm) maintained at 40 °C. The mobile phase comprised (A) 10 mM ammonium acetate (pH 9.0) and (B) acetonitrile. The gradient elution program was set as follows: 90% to 60% B over 10 min at a flow rate of 0.2 ml/min, followed by a 7-min re-equilibration period. The injection volume ranged from

2 to 5 μL. MS detection used positive ESI mode with MRM acquisition. Source conditions were set as follows: gas temperature 300 °C, gas flow 5 L/min, nebulizer pressure 45 psi, and capillary voltage 3500 V. Quantitation was achieved using a stable isotope-labeled internal standard. Quality control samples were regularly interspersed throughout the analytical sequence. Data were processed with MassHunter Quant software.

Polar metabolites analysis by GC-MS.

Following acyl-CoA analysis, samples underwent vacuum centrifugation to complete dryness. Derivatization was initiated by reconstituting residues in methoxylamine hydrochloride solution (10 mg/ml) with a 30-minute incubation at room temperature. Subsequently, N-methyl-N-(tert-butyldimethylsilyl) trifluoroacetamide (MTBSTFA) was added and samples were heated at 70° C for 1 hour. Chromatographic separation was achieved using an Agilent 5975C GC-MS system equipped with a DB-5MS + DG capillary column (30 m × 250 μm × 0.25 μm). The injection port was maintained at 280° C and operated in splitless mode with 1 μL injections. The temperature program commenced at 60℃ (1 min hold), followed by a 10° C/min ramp to 320° C, with a final 10-minute hold. Helium carrier gas flow was optimized for metabolite separation. The mass spectrometer interface and quadrupole were maintained at 285° C and 150° C, respectively, with electron impact ionization at 70 eV. Mass spectrometric detection incorporated both full scan (50-700 m/z) and selected ion monitoring modes. Quantification was based on characteristic M-57 fragment ions using Agilent MassHunter Quantitation software, with metabolite identification verified against

306 authentic standards through retention time and mass spectral matching.

307 **Immunofluorescence**

308 After washing with precooled PBS, cells were fixed in 4% paraformaldehyde and
309 permeabilized with 0.5% Triton X-100. They were then blocked with fetal bovine
310 serum. Following removal of the blocking solution, cells were incubated with
311 fluorescent-conjugated primary antibody overnight at 4 °C. The next day, cells were
312 washed with PBS containing 0.1% Tween 20 and PBS, then incubated with secondary
313 antibody for 1 hour. Nuclei were stained with DAPI, and images were acquired using a
314 laser scanning confocal microscope (Olympus FV3000).

315 **Co-immunoprecipitation**

316 For co-IP analysis, cells were lysed in 500 μl of lysis buffer (50 mM Tris-Cl pH 7.4, 1
317 mM EDTA, 0.2% Triton X-100, protease inhibitor) on ice for 30 min. After
318 centrifugation, 50 μl of the supernatant was kept as input for the western blot. The rest
319 lysate was incubated with the corresponding antibody at 4 ℃ overnight, followed by
320 incubation with protein A/G agarose beads (Santa Cruz Biotech., sc-2003) for 3 h. Then,
321 the beads/protein complex was washed 5 times with cold lysis buffer and boiled with
322 40 μl of SDS loading buffer, and analyzed by western blot.

323 **Human study and approval**

324 The MAFLD patients recruited from Changzhou No. 2 People's Hospital were
325 diagnosed by ultrasonography and serologic testing. Inclusion criteria were as follows:
326 1) age between 18 and 65 years; 2) clinical diagnosis of non-alcoholic fatty liver (NAFL)
327 or non-alcoholic steatohepatitis (NASH); 3) provision of written informed consent.

Exclusion criteria included: 1) severe comorbidities affecting major organs (e.g., heart, liver, or kidney); 2) history of malignant tumors; 3) pregnancy or lactation; 4) psychiatric disorders. The liver tissue samples of patients were obtained intraoperatively from bariatric surgery, and subjects with excessive alcohol intake or other liver diseases (such as viral hepatitis and drug damage et al.) were excluded. Adjacent non-cancer normal liver tissues were collected from liver cancer surgical resection as normal control liver specimens, except those with metabolic abnormalities. The study was approved by the Ethics Committee of the Changzhou No. 2 People's Hospital and followed the ethical guideline Declaration of Helsinki. Written informed consent was provided by each subject ([2023]KY124-01).

Animal

Association for Assessment and Accreditation of Laboratory Animal Care International has accredited the animal experimental center. Animals received human care following the National Institutes of Health's Guide to the Care and Use of Laboratory Animals. All animal experiments and care were approved by the Animal Ethics Committee of China Pharmaceutical University (2024-06-017). Male C57BL/6J wild-type mice, ob/ob mice, and littermate controls (SPF grade, 6-7 weeks old, 20 to 22 g) were obtained from GemPharmatech Co. Ltd (Nanjing, China). Animals were maintained on a 12-h light-dark cycle at 22-24℃ and had free access to water and Normal chow (Jiangsu synergetic biology Co., Ltd, 1010039) unless otherwise stated.

Diet-induced mouse MAFLD models

High-fat diet-induced mouse MAFLD models were constructed by feeding mice an

HFD diet (60 kcal% fat, 20.6 kcal% carbohydrate,19.4 kcal% protein) for 8, 16, or 32 weeks. FPC diet-induced mouse MAFLD models were constructed by feeding mice an FPC diet (52 kcal% fat, 34.5 kcal% sucrose, and 1.25% cholesterol; Teklad, TD190142) combined with 42 g/L sugar solution (55% glucose + 45% fructose) in drinking water for 16 weeks. HFrD diet-induced mouse MAFLD models were constructed by feeding mice an HFrD diet (10 kcal% fat and 60 kcal% fructose; Research Diets, Inc. D02022704K) for 6 weeks. AMLN diet-induced mouse MAFLD models were constructed by feeding mice an AMLN diet (40 kcal% fat, 20 kcal% fructose and 2% cholesterol; Research Diets, D09100310) for 16 weeks.

Diet-induced mouse MASH models

A mouse MASH model was built by feeding mice an HFMRCD diet (60 kcal% fat with low methionine and no Choline; Xietong Shengwu, XTMRCD-60) for 6 weeks. Another mouse MASH model was built by feeding mice an FPC diet (52 kcal% fat, 34.5 kcal% sucrose, and 1.25% cholesterol; Teklad, TD190142) combined with 42 g/L sugar solution (55% glucose + 45% fructose) in drinking water for 24 weeks.

AAV8-mediated gene overexpression

For AAV8 transduction, mice were fed 4-7 weeks of HFD and then injected with 2.5e11 VG of AAV-*LacZ*/AAV-*KAT2A* WT/AAV-*KAT2A* Mut or AAV-m-SREBP1c through the tail vein. The thyroxine-binding globulin (TBG) promoter was adopted for hepatocyte-specific expression.

Generation of *Kat2a*^{HKO} mice

Hepatocyte-specific *Kat2a* knockout (*Kat2a*^{HKO}) mice were established with the

CRISPR-Cas9 system and Cre-loxP-mediated recombination technology. *Kat2a*$^{fl/fl}$ mice and Albumin-Cre (Alb-Cre) mice were obtained from GemPharmatech Co. Ltd (Nanjing, China). All the mice were C57BL/6 J background. *Kat2a*^{HKO} mice were generated by crossing homozygous *Kat2a*$^{fl/fl}$ mice with Alb-Cre mice. Exon 7-11 of *Kat2a* in hepatocytes were depleted from *Kat2a*$^{fl/fl}$ mice. PCR was applied for genotyping using DNA extracted from mouse tails. The genotyping primers were as follows:

Kat2a-F, 5'-AAGTGAAGCCATTACCTATCTCTGTGCC-3';

Kat2a-R, 5'-GCCAGGATAGAGACTGGAGACCCAA-3';

Cre-F, 5'-GGGCAGTCTGGTACTTCCAAGCT-3';

Cre-R, 5'-TAGCTACCTATGCGATCCAAACAAC-3';

WT-F, 5'-CAGCAAAACCTGGCTGTGGATC-3';

WT-R, 5'-ATGAGCCACCATGTGGGTGTC-3'.

The primer pairs *Kat2a*-F and *Kat2a*-R were used to detect flox allele (wildtype allele = 257 bp, flox allele = 359 bp). The primer pairs Cre-F and Cre-R were used to detect the Alb-Cre allele (Alb-Cre allele = 340 bp; wildtype allele = None). The primer pairs WT-F and WT-R were used to detect whether Alb-Cre mice were homozygous or heterozygous (homozygote = None; heterozygote = 412 bp).

Measurement of *de novo* lipogenesis by ^{13}C fructose gavage

To measure lipogenesis with ^{13}C-fructose gavage, *Kat2a*^{HKO} and *Kat2a*$^{fl/fl}$ mice were fed an HFD diet for 11 days or FPC diet for 9 days. After a 10-hour fast, mice were refed for 2 hours, and received oral gavage (2g/kg) with a 1:1 mixture of ^{12}C D-glucose

and ^{13}C fructose. Mice were sacrificed, and livers were collected and snap-frozen in liquid nitrogen in the following day. Lipids were extracted from 20 mg of liver tissue through saponification and analyzed via LC-MS as previously described. Signal intensities were obtained for each fatty acid isotopomer (M+i), where M denotes the unlabeled parent ion and i represents the number of ^{13}C atoms incorporated (ranging from 0 to n, n being the total carbon number of the fatty acid). The fractional enrichment was calculated as follows: for each fatty acid, the intensity of each isotopomer was multiplied by i, summed across all isotopomers, divided by n and the total ion count, and multiplied by 100 to obtain percentage enrichment.

Measurement of *de novo* lipogenesis by $^{2}H_2O$ injection

To measure lipogenesis with ^{13}C-fructose gavage, *Kat2a*^{HKO} and *Kat2a*$^{fl/fl}$ mice were fed an HFD diet for 11 days or FPC diet for 9 days. Following the feeding period, mice received an intraperitoneal injection (30 μL/g) of 99.9% $^{2}H_2O$ (Sigma-Aldrich, 151882) in 0.9% NaCl. Five hours post-injection, the mice were euthanized, and livers were collected and snap-frozen in liquid nitrogen. Lipids were extracted from 20 mg of frozen liver tissue via saponification and analyzed by LC-MS as described. Ion counts were acquired for each fatty acid isotopomer (M+i), where M represents the unlabeled parent ion and i corresponds to the number of incorporated deuterium atoms (ranging from 0 to n, n being the total number of hydrogen atoms in the fatty acid eligible for labeling). Deuterium enrichment was calculated as follows: for each fatty acid, the intensity of each isotopomer was multiplied by i, summed over all isotopomers, divided by n and the total ion count, and multiplied by 100 to obtain percentage enrichment.

CPTH2 treatment

Male C57BL/6J wild-type mice (8 weeks old) were fed 4 weeks of HFD diet or 10 weeks of FPC diet. Then mice were treated with vehicle A (10% DMSO, 40% PEG3000, 5% Tween-80, 45% saline, v/v) or CPTH2 (20 mg/kg) in vehicle A by intragastric gavage every day, along with HFD fed. After another 6 weeks, mice were euthanized for analysis.

CPTH2 and T0901317 treatment

Male C57BL/6J wild-type mice (8 weeks old) were fed 6 weeks of HFD**.** Then mice were treated with vehicle A/ T0901317 (0.5 mg/kg)/ CPTH2 (20 mg/kg) or T0901317 and CPTH2 in the vehicle by intragastric gavage every day, along with HFD fed. After another 2 weeks, mice were euthanized for analysis.

Histological analysis of liver

Livers were fixed in 4% paraformaldehyde at 4°C overnight, embedded in paraffin wax, and sectioned into 5 μm thickness slices. Liver sections were stained with hematoxylin and eosin (H&E) staining to estimate morphology. Liver sections were stained by oil red O and counterstained with hematoxylin to evaluate lipid accumulation. Liver sections were stained by Sirius Red to assess liver fibrosis. The indicated antibodies were applied for Immunohistochemistry (IHC) staining. The sections were observed and captured using an upright fluorescence microscope (Olympus, BX53, Tokyo, Japan). The lipid drops were quantified by ImageJ (Version 1.5a).

Quantification and Statistical Analysis

Data were analyzed using GraphPad Prism (Version 8). All data are represented as mean

± SEM. Statistical significance was analyzed by the student's t-test between the two groups. When comparison between three or more groups, one-way ANOVA or two-way ANOVA was used. The D'agostino-Pearson normal test was used to determine whether the data conformed to normal distribution. A $p<0.05$ was considered as statistically significant (*P < 0.05, **P < 0.01, ***P < 0.001, ns = not significant).

Figure S1. Hepatocyte GCN5 is induced by PAOA conditions via KLF15.

(A-C) Simple linear regression analysis revealed a significant correlation between hepatic GCN5 and PCAF expression levels with the levels of bile acid (A), glucose (B), and insulin (C). (D-L) Hepatocytes were incubated with PA (200 μM) and OA (400 μM) at indicated times (n=3). The protein levels of GCN5 and PACF were detected by western blot in HL-7702 (D, E), HepG2 (G, H), and mouse primary hepatocytes (J, K). The mRNA levels of *KAT2A* and *KAT2B* were detected by qRT-PCR in HL-7702 (F), HepG2 (I), and mouse primary hepatocytes (L) (n=6). (M) Prediction of KAT2A-promoter-binding TFs. (N) Relative luciferase activity of the luciferase reporter plasmid containing KAT2A promoter in HL-7702 hepatocytes transfected with the plasmids overexpressing the four predicted transcription factors and the control plasmid, and then treated with PAOA for 24 h (n=6). (O) Relative mRNA levels of *KAT2A* in HL-7702 hepatocytes transfected with the indicated plasmids after treated with PAOA for 24 h (n=6). (P) Relative enrichment of Flag-KLF15 on the indicated regions of KAT2A promoter in HL-7702 hepatocytes detected by ChIP assay using anti-Flag or control IgG antibody, combined with qPCR assay (n=6). (Q) Relative luciferase activity of luciferase reporter plasmids containing wild-type KAT2A promoter (WT) or its mutant (MUT) in HL-7702 hepatocytes transfected with the plasmids overexpressing KLF15 or the control plasmid and then treated with PAOA for 12 h (n=6). The upper sequences show KLF15 binding motif (blue) and its mutant (red). Error bars are represented as mean ± SEM. Statistical analysis was done with one-way ANOVA (Dunnett's post-test; E, F, H, I, K, L, N, O and Q) and two-way ANOVA (Sidak's multiple comparisons test;

P). *p < 0.05, **p < 0.01, ***p < 0.001 *vs* Control (E, F, H, I, K and L), Flag (N, O), IgG (P), or WT/Flag (Q).

Figure S2. Validation of hepatocyte-specific overexpression of GCN5 in MAFLD mice.

(A) The protein expression of GCN5 and PCAF in the heart, kidney, spleen, and lung were detected by western blot (n=4). (B) The mRNA levels of *Kat2a* and *Kat2b* in the liver were detected by qRT-PCR (n=6). (C) Food intake. (D) Body weight. (E) Quantification analyses of drop lipids in the liver were performed by ImageJ (n=6). (F) The protein expression of GCN5 and PCAF in the heart, kidney, spleen, and lung were detected by western blotting validation (n=4). (G) The mRNA levels of *Kat2a* and *Kat2b* in the liver were detected by qRT-PCR (n=3). (H) Food intake. (I) Body weight. (J) Quantification analyses of drop lipids in the liver were performed by ImageJ (n=6). (K-M) The overexpression of *KAT2A* WT *and KAT2A* MUT (E575Q) plasmids were validated by western blot in HL-7702 (K), HepG2 (L), and mouse primary hepatocytes (M) (n=3). Error bars are represented as mean ± SEM. Statistical analysis was done with two-way ANOVA (Sidak's multiple comparisons test; B-E and G-J). *p < 0.05, **p < 0.01, ***p < 0.001 *vs* AAV-*LacZ* (A-J), or Vehicle (K-M).

Figure S3. Validation of hepatocyte-specific knockout of GCN5 in HFD diet.

(A) Schematic depiction of the generation of *Kat2a* hepatocyte-specific knockout mice ($Kat2a^{HKO}$) and the control mice ($Kat2a^{fl/fl}$). (B) Genotyping of the $Kat2a^{HKO}$ and $Kat2a^{fl/fl}$ mice. (C) The protein expression of GCN5 and PCAF in the heart, kidney, spleen, and lung were detected by western blot (n=4). (D-G) HFD diet. (D) The mRNA

489 levels of *Kat2a* and *Kat2b* in the liver were detected by qRT-PCR (n=6). (E) Food intake.
490 (F) Body weight. (G) Quantification analyses of drop lipids in the liver were performed
491 by ImageJ (n=6). Error bars are represented as mean ± SEM. Statistical analysis was
492 done with student's *t*-test (G), and two-way ANOVA (Sidak's multiple comparisons test;
493 D-F). *p < 0.05, **p < 0.01, ***p < 0.001 *vs* $Kat2a^{f/f}$.

494 **Figure S4. Liver-specific KO of GCN5 protects mice from HFrD diet-induced**
495 **MAFLD.**

496 (A) Schematic diagram of HFrD diet-induced MAFLD models in $Kat2a^{HKO}$ and
497 $Kat2a^{fl/fl}$ mice. (B) Successful depletion of GCN5 protein in the liver was verified by
498 western blot (n=3). (C) LW and LW/BW of $Kat2a^{HKO}$ and $Kat2a^{fl/fl}$ mice (n=6). (D)
499 Representative H&E and Oil Red O staining of the liver (n=6). (E) The levels of serum
500 TG, TC, HDL-c, and LDL-c (n=6). (F) The contents of liver TG and TC (n=6). (G) The
501 levels of serum AST and ALT (n=6). (H) The mRNA levels of *Kat2a* and *Kat2b* in the
502 liver were detected by qRT-PCR (n=6). (I) Food intake. (J) Body weight. (K)
503 Quantification analyses of drop lipids. Statistical analysis was done with student's t-test
504 (C-G and K), one-way ANOVA (Dunnett's post-test; H), and two-way ANOVA (Sidak's
505 multiple comparisons test; I and J). *p < 0.05, **p < 0.01, ***p < 0.001 vs $Kat2a^{f/f}$.

506 **Figure S5. Liver-specific KO of GCN5 protects mice from AMLN diet-induced**
507 **MAFLD.**

508 (A) Schematic diagram of AMLN diet-induced MAFLD models in $Kat2a^{HKO}$ and
509 $Kat2a^{fl/fl}$ mice. (B) Successful depletion of GCN5 protein in the liver was verified by
510 western blot (n=3). (C) LW and LW/BW of $Kat2a^{HKO}$ and $Kat2a^{fl/fl}$ mice (n=6). (D)

Representative H&E and Oil Red O staining of the liver (n=6). (E) The levels of serum TG, TC, HDL-c, and LDL-c (n=6). (F) The contents of liver TG and TC (n=6). (G) The levels of serum AST and ALT (n=6). (H) The mRNA levels of *Kat2a* and *Kat2b* in the liver were detected by qRT-PCR (n=6). (I) Food intake. (J) Body weight. (K) Quantification analyses of drop lipids. Statistical analysis was done with student's t-test (C-G and K), one-way ANOVA (Dunnett's post-test; H), and two-way ANOVA (Sidak's multiple comparisons test; I and J). *p < 0.05, **p < 0.01, ***p < 0.001 vs $Kat2a^{f/f}$.

Figure S6. Validation of hepatocyte-specific knockout of GCN5 in FPC diet and HFMRCD diet.

(A-G) FPC diet. (A) The mRNA levels of *Kat2a* and *Kat2b* in the liver were detected by qRT-PCR (n=6). (B) Food intake. (C) Body weight. (D-G) Quantification analyses of drop lipids of 16w (D) and 24w (E), Sirius Red (F), and F4/80 (G) of the liver were performed by ImageJ (n=6). (H-N) HFMRCD diet. (H) The mRNA levels of *Kat2a* and *Kat2b* in the liver were detected by qRT-PCR (n=6). (I) Food intake. (J) Body weight. (K-M) Quantification analyses of drop lipids (K), Sirius Red (L), and F4/80 (M) of the liver were performed by ImageJ (n=6). (N) The indicated protein levels in liver tissue were detected by western blot (n=3). Error bars are represented as mean ± SEM. Statistical analysis was done with student's *t*-test (D-G and K-M), and two-way ANOVA (Sidak's multiple comparisons test; A-C and H-J). *p < 0.05, **p < 0.01, ***p < 0.001 *vs* $Kat2a^{f/f}$.

Figure S7. Hepatocyte GCN5 knockout reduces PAOA-induced lipid accumulation in vivo.

(A-F) *KAT2A* KO hepatocytes were transfected with *KAT2A* WT and *KAT2A* MUT (E575Q) plasmids for 12 h, then the cells were incubated with PA (200 μM) and OA (400 μM) for 24 h. (A-B) The replenishment of *KAT2A* KO cells with *KAT2A* WT and *KAT2A* MUT plasmids was validated by western blot (A) and qRT-PCR (B) (n=3). (C)The cellular TG and TC levels were detected (n=3). (D-E) The lipids were stained with Bodipy (D) and Nile red (E) (n=6). (F) Quantification analyses of intracellular neutral lipids by ImageJ (n=6). Statistical analysis was done with one-way ANOVA (Dunnett's post-test; B, C and F). *p < 0.05, **p < 0.01, ***p < 0.001 vs BSA-WT+Vector.

Figure S8. Validation of CPTH2.

(A) The mean plasma concentration-time curve of CPTH2. (B) The mean tissue distributions of CPTH2 in liver, heart, spleen, lung, kidney, muscle, WAT, BAT and brain. (C) The protein expression of GCN5 and PCAF in the heart, kidney, spleen, and lung were detected by western blotting validation (n=4). (D-F) HFD diet. (D) Food intake. (E) Body weight. (F) Quantification analyses of drop lipids in the liver were performed by ImageJ (n=5). (G-I) FPC diet. (G) Body weight. (H) Food intake. (I) Quantification analyses of drop lipids in the liver were performed by ImageJ (n=8). Statistical analysis was done with student's t-test (F, I), and two-way ANOVA (Sidak's multiple comparisons test; D, E, G, H). *p < 0.05, **p < 0.01, ***p < 0.001 vs Vehicle.

Figure S9. CPTH2 reduces PAOA-induced lipid accumulation in vivo.

(A-C) HL-7702, HepG2, and mouse primary hepatocytes were treated with increasing concentrations of CPTH2 for 24 h, and cell viability was assessed by MTT (n=6). (D-

L) HL-7702, HepG2 and mouse primary hepatocytes were incubated PA (200 μM) and OA (400 μM) with CPTH2 (25 or 50 μM) for 24 h, then stained with Nile Red and Bodipy (D, G, and J). Quantification of the cellular lipids was analyzed by ImageJ (E, H and K) (n=6). The cellular TG and TC levels (F, I and L) (n=3). Error bars are represented as mean ± SEM. Statistical analysis was done with one-way ANOVA (Dunnett's post-test; A-L). *p < 0.05, **p < 0.01, ***p < 0.001 *vs* Vehicle (A-C), or PAOA (D-L).

Figure S10. Effect of CPTH2 on hepatic lipid metabolism.

(A) Schematic illustration of intermediate metabolites and genes involved in glycolysis/gluconeogenesis, FA synthesis, glyceroneogenesis, and triacylglyceride synthesis. (B-D) RNA sequencing was performed on *KAT2A* KO HL-7702 cells and HL-7702 cells treated with PAOA (n=3). (B) Volcano plot representation of significantly up-and down-regulated genes. (C) Gene Ontology analysis. (D) Gene Set Enrichment Analysis plot of enrichment. (E) Body weight in Figure 5P. (F) Body weight in Figure 5R. (G) The *de novo* lipogenesis was measured in the HL-7702 cells (n=5). (H) Oxygen consumption rate (OCR) was measured in the HL-7702 cells (n=5). (I) Fatty acid uptake was measured in the HL-7702 cells (n=5). Error bars are represented as mean ± SEM. Statistical analysis was done with a student's *t*-test. *p < 0.05, **p < 0.01, ***p < 0.001 *vs* $Kat2a^{fl/fl}$ or *KAT2A WT.*

Figure S11. Overexpression of GCN5 promotes hepatic DNL by increasing SREBP1 level.

(A-C) HL-7702 cells were transfected with the indicated plasmids for 12 h, and cultured

in medium B for 24 h (n=3). (A) The luciferase activity of indicated genes was measured. (B) The indicated protein levels were detected by western blot. (C) The indicated gene expression was detected by qRT-PCR. (D-F) *KAT2A* KO HL-7702 cells were cultured in medium B for 24 h (n=3). (D) The luciferase activity of indicated genes was measured. (E) The indicated protein levels were detected by western blot. (F) The indicated gene expression was detected by qRT-PCR. (G-I) HL-7702 cells were treated with CPTH2 (50 μM) in medium B for 24 h (n=3). (G) The luciferase activity of indicated genes was measured (n=3). (H) The indicated protein levels were detected by western blot. (I) The indicated gene expression was detected by qRT-PCR. (J-L) *KAT2A* KO HL-7702 cells were transfected with *KAT2A* WT and *KAT2A* MUT (E575Q) plasmids for 12 h, treated with CPTH2 (50 μM) in medium B for 24 h (n=3). (J) The luciferase activity of indicated genes was measured. (K) The indicated protein levels were detected by western blot. (L) The indicated gene expression was detected by qRT-PCR. (M) *KAT2A* KO HL-7702 cells were transfected with mSREBP1c plasmids for 12 h and incubated with PAOA for 24 h. The indicated gene expression was detected by qRT-PCR (n=3). (M) Simple linear regression analysis revealed a significant correlation of hepatic GCN5 expression levels with SREBP1 expression levels in MAFLD patients. Error bars are represented as mean ± SEM. Statistical analysis was done using the student's *t*-test (D-L) and one-way ANOVA (Dunnett's post-test; A and C). *$p < 0.05$, **$p < 0.01$, ***$p < 0.001$.

Figure S12. Loss of GCN5 reduces PAOA-induced lipid accumulation by SREBP1c pathway in vivo.

(A-E) *KAT2A* KO HL-7702 cells were transfected with pSREBP1c or mSREBP1c plasmids for 12 h and incubated with PAOA for 24 h. (A)the indicated protein levels were detected by western blot (n=3). (B) The cellular lipids were stained with Nile Red and Bodipy. (C) Quantification of the cellular lipids was analyzed by ImageJ (n=6). (D) The indicated gene expression was detected by q-PCR (n=3). (E) The cellular TG and TC levels (n=3). (F-M) HepG2 and primary hepatocyte cells were transfected with pSREBP1c or mSREBP1c plasmids for 12 h, then treated with CPTH2 (50 μM) and PAOA in medium B for 24 h. (F) The indicated protein levels were detected by western blot (n=3). (G) The indicated gene expression was detected by q-PCR (n=3). (H-I) The cellular TG and TC levels of HepG2 (H) and primary hepatocytes (I) (n=3). (J-M) The HepG2 (J) and primary hepatocytes (K) cellular lipids were stained with Nile red and Bodipy. Quantification of the cellular lipids was analyzed by ImageJ of HepG2 (L) and primary hepatocytes (M) (n=6). Statistical analysis was done using one-way ANOVA. *p < 0.05, **p < 0.01, ***p < 0.001.

Figure S13. Body weight and food intake in *Kat2a*^{HKO} and *Kat2a*$^{fl/fl}$ mice with overexpressing mSREBP1c

(A-B) HFD diet. (A) Body weight. (B) Food intake. (C-D) FPC diet. (C) Body weight. (D) Food intake. Statistical analysis was done using two-way ANOVA (Sidak's multiple comparisons test). *p < 0.05, **p < 0.01, ***p < 0.001.

Figure S14. The expression of H3K9ac and H3K14ac in MAFLD and their relevance to GCN5.

(A) HL-7702 cells were transfected with Myc-*tag* GCN5 and Flag-*tag*-SREBP1c

plasmids for 12 h, and treated with CPTH2 for 24 h. The acetylation level of SREBP1c and the interaction of GCN5 and SREBP1c were detected by IP (n=3). (B-C) HL-7702 cells were incubated with 100 μM cycloheximide for 1 h, afterwards, the cells were supplemented with 50 μM cycloheximide plus vehicle, or CPTH2 for the indicated time. The protein levels of SREBP1 were detected by WB (B), quantification of SREBP1 protein levels (C) (n=3). (D-E) Simple linear regression analysis revealed a significant correlation between hepatic GCN5 expression levels with the levels of H3K9ac (D), and H3K14ac (E) in MAFLD patients. (F-K) The protein levels of H3K9ac and H3K14ac in the fatty liver of HFD-induced mice (F), ob/ob mice (G), PAOA-induced HL-7702 (H), *KAT2A* KO HL-7702 cells (I), HL-7702 cells treated with CPTH2 (J), and HL-7702 cells transfected with *KAT2A* WT (K) (n=3). Error bars are represented as mean ± SEM. Statistical analysis was done with two-way ANOVA (Dunnett's post-test). *p < 0.05, **p < 0.01, ***p < 0.001.

Figure S15. GCN5 does not influence ABCA1 expression in a ligand-dependent manner via LXRE.

(A) Schematic diagram of primer locations used for the ChIP assay across the *ABCA1* genomic structure. (B-C) HL-7702 cells were transfected with LXRα/RXRα/GCN5, and a luciferase reporter plasmid under the control of *ABCA1* WT promoter (B), *ABCA1* Mutant promoter (C), incubated with T0901317 and GW3965 (n=3). (D) AlphaFold 3 predicted structure of GCN5 (yellow) interact with LXRα (green). Hydrogen bonds are shown as red dashed lines. (E-F) HL-7702 cells were transfected with siRNAs for 48 h. The cells were incubated with T0901317 and GW3965 for 24 h. ChIP assays were

643 performed with anti-GCN5 (E) or anti-H3K9ac (F) antibodies. Recruitment of GCN5
644 and H3K9ac to the LXREs of the *ABCA1* genes was determined by qRT-PCR (n=3).
645 (G) The mRNA expression of *LXRα* was detected by qRT-PCR (n=3). (H-I) *KAT2A* KO
646 HL-7702 cells were treated with T0901317 and GW3965 for 24 h. ChIP assays were
647 performed with anti-LXRα (H) or anti-H3K9ac (I) antibodies. Recruitment of LXRα
648 and H3K9ac to the LXREs of the *ABCA1* genes was determined by qRT-PCR (n = 3).
649 Error bars are represented as mean ± SEM. Statistical analysis was done with student's
650 *t*-test (G) and one-way ANOVA (Dunnett's post-test; B-F and H-I,). *p < 0.05, **p <
651 0.01, ***p < 0.001.

652 **Figure S16. CPTH2 does not influence T0901317-induced RCT.**

653 (A-B) The primary hepatocyte cells were incubated PAOA with indicated compounds
654 (T091317, GW3965, or CPTH2) for 24 h. (A) The treated cells were stained with Nile
655 Red and Bodipy. (B) Quantification of the cellular lipids was analyzed by ImageJ (n=6).
656 (C) Quantification of the HL-7702 cellular lipids was analyzed by ImageJ (n=6). (D)
657 Food intake. (E) Body weight. (F) Graphical abstract. Error bars are represented as
658 mean ± SEM. Statistical analysis was done with student's t-test (B), one-way ANOVA
659 (Dunnett's post-test; A), and two-way ANOVA (Sidak's multiple comparisons test; D
660 and E). *p < 0.05, **p < 0.01, ***p < 0.001.
661

Figure S1

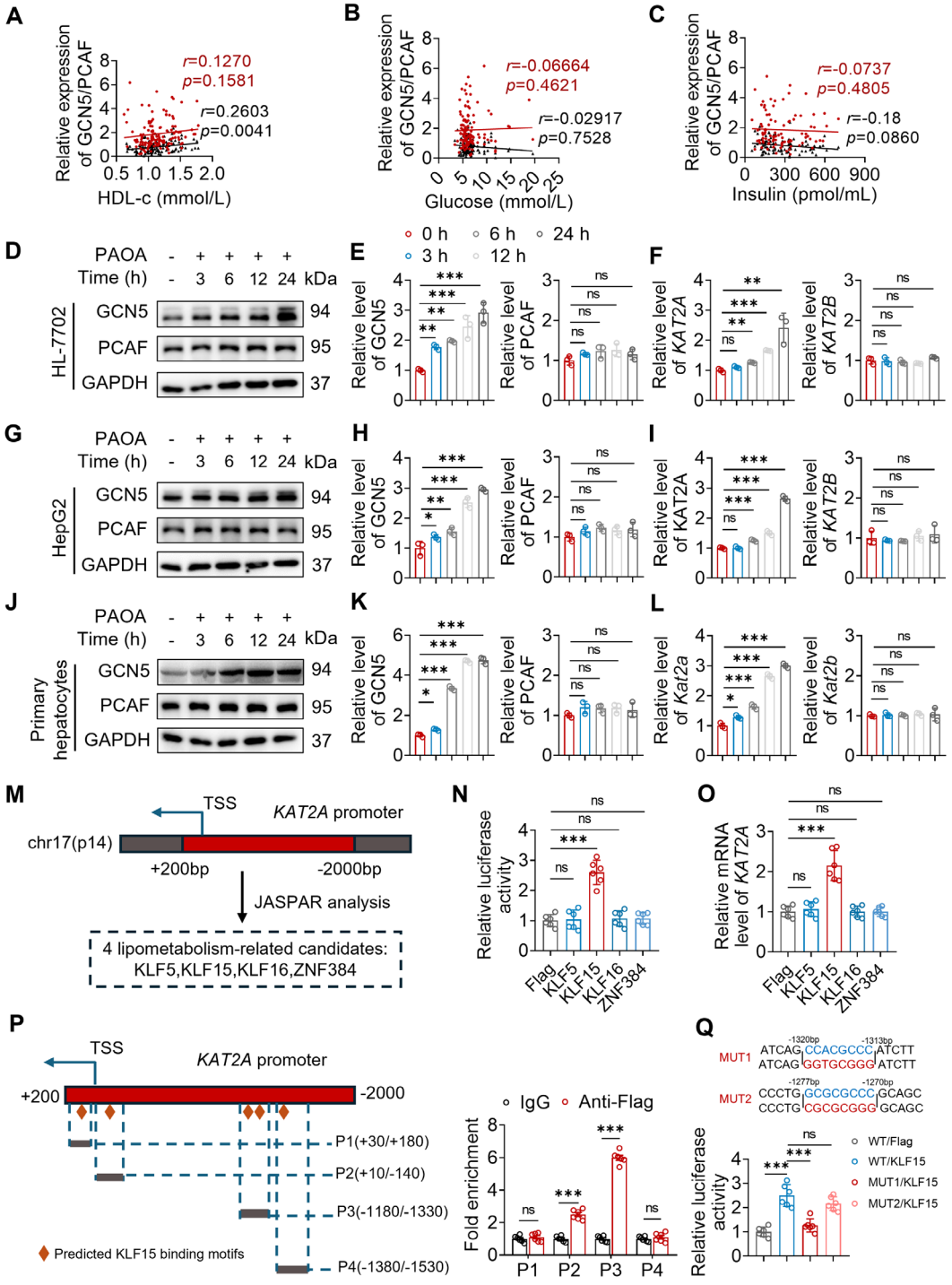
A
Relative expression of GCN5/PCAF
r=0.1270
p=0.1581
r=0.2603
p=0.0041
HDL-c (mmol/L)
B
r=-0.06664
p=0.4621
r=-0.02917
p=0.7528
Glucose (mmol/L)
C
r=-0.0737
p=0.4805
r=-0.18
p=0.0860
Insulin (pmol/mL)
D
PAOA
Time (h)
HL-7702
GCN5
PCAF
GAPDH
kDa
E
0 h
3 h
6 h
12 h
24 h
Relative level of GCN5
Relative level of PCAF
F
Relative level of KAT2A
Relative level of KAT2B
G
HepG2
H
I
J
Primary hepatocytes
K
Relative level of Kat2a
Relative level of Kat2b
L
M
TSS
KAT2A promoter
chr17(p14)
+200bp
-2000bp
JASPAR analysis
4 lipometabolism-related candidates:
KLF5,KLF15,KLF16,ZNF384
N
Relative luciferase activity
Flag
KLF5
KLF15
KLF16
ZNF384
O
Relative mRNA level of KAT2A
P
+200
-2000
P1(+30/+180)
P2(+10/-140)
P3(-1180/-1330)
P4(-1380/-1530)
Predicted KLF15 binding motifs
IgG
Anti-Flag
Fold enrichment
P1
P2
P3
P4
Q
MUT1
ATCAG CCACGCCC ATCTT
ATCAG GGTGCGGG ATCTT
MUT2
CCCTG GCGCGCCC GCAGC
CCCTG CGCGCGGG GCAGC
WT/Flag
WT/KLF15
MUT1/KLF15
MUT2/KLF15

Figure S2

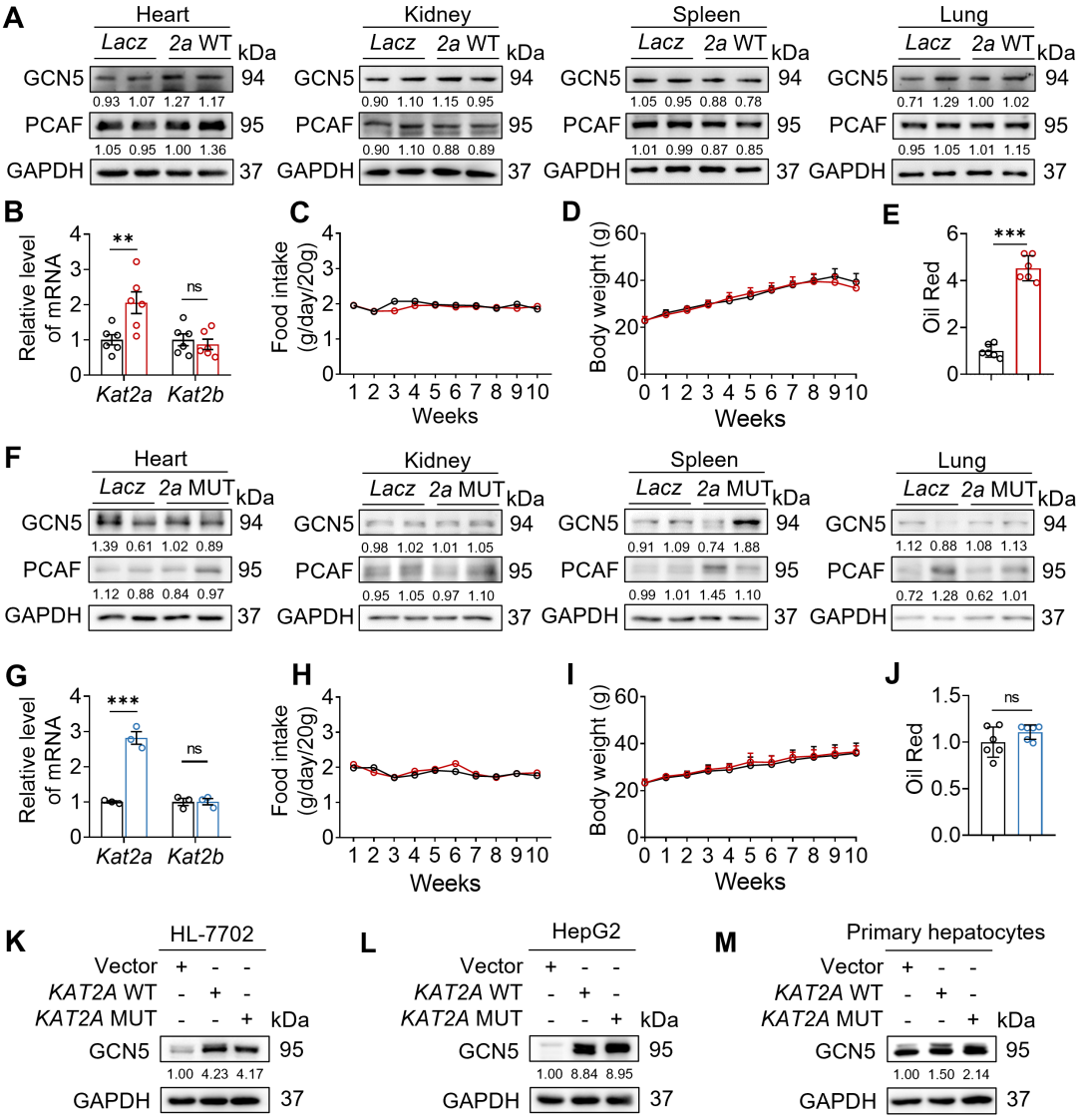
A
Heart
Kidney
Spleen
Lung
Lacz
2a WT
kDa
GCN5
PCAF
GAPDH
94
95
37
0.93 1.07 1.27 1.17
1.05 0.95 1.00 1.36
0.90 1.10 1.15 0.95
0.90 1.10 0.88 0.89
1.05 0.95 0.88 0.78
1.01 0.99 0.87 0.85
0.71 1.29 1.00 1.02
0.95 1.05 1.01 1.15
B
Relative level of mRNA
**
ns
Kat2a
Kat2b
C
Food intake (g/day/20g)
Weeks
D
Body weight (g)
Weeks
E
Oil Red
***
F
Heart
Kidney
Spleen
Lung
Lacz
2a MUT
kDa
GCN5
PCAF
GAPDH
94
95
37
1.39 0.61 1.02 0.89
1.12 0.88 0.84 0.97
0.98 1.02 1.01 1.05
0.95 1.05 0.97 1.10
0.91 1.09 0.74 1.88
0.99 1.01 1.45 1.10
1.12 0.88 1.08 1.13
0.72 1.28 0.62 1.01
G
Relative level of mRNA
***
ns
Kat2a
Kat2b
H
Food intake (g/day/20g)
Weeks
I
Body weight (g)
Weeks
J
Oil Red
ns
K
HL-7702
Vector
KAT2A WT
KAT2A MUT
kDa
GCN5
95
1.00 4.23 4.17
GAPDH
37
L
HepG2
Vector
KAT2A WT
KAT2A MUT
kDa
GCN5
95
1.00 8.84 8.95
GAPDH
37
M
Primary hepatocytes
Vector
KAT2A WT
KAT2A MUT
kDa
GCN5
95
1.00 1.50 2.14
GAPDH
37

Figure S3

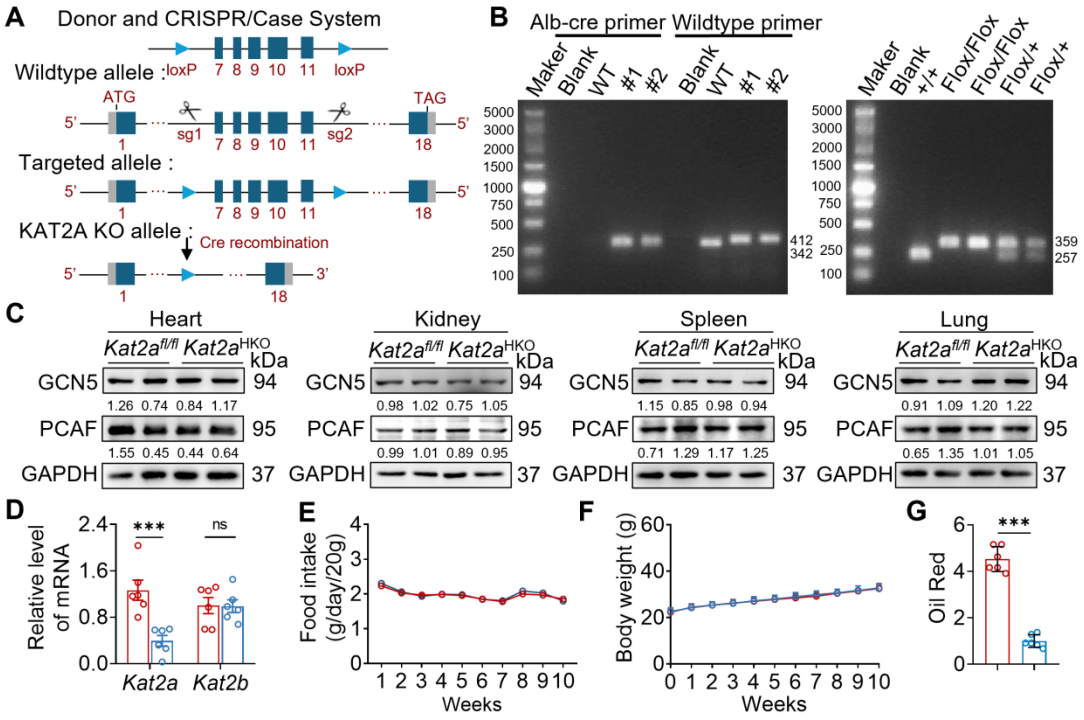
A
Donor and CRISPR/Case System
Wildtype allele :
loxP 7 8 9 10 11 loxP
ATG
TAG
sg1
sg2
Targeted allele :
KAT2A KO allele :
Cre recombination
B
Alb-cre primer
Wildtype primer
Maker
Blank
WT
#1
#2
+/+
Flox/Flox
Flox/+
C
Heart
Kidney
Spleen
Lung
Kat2afl/fl
Kat2aHKO
kDa
GCN5
PCAF
GAPDH
D
Relative level of mRNA
Kat2a
Kat2b
ns
E
Food intake (g/day/20g)
Weeks
F
Body weight (g)
Weeks
G
Oil Red

Figure S4

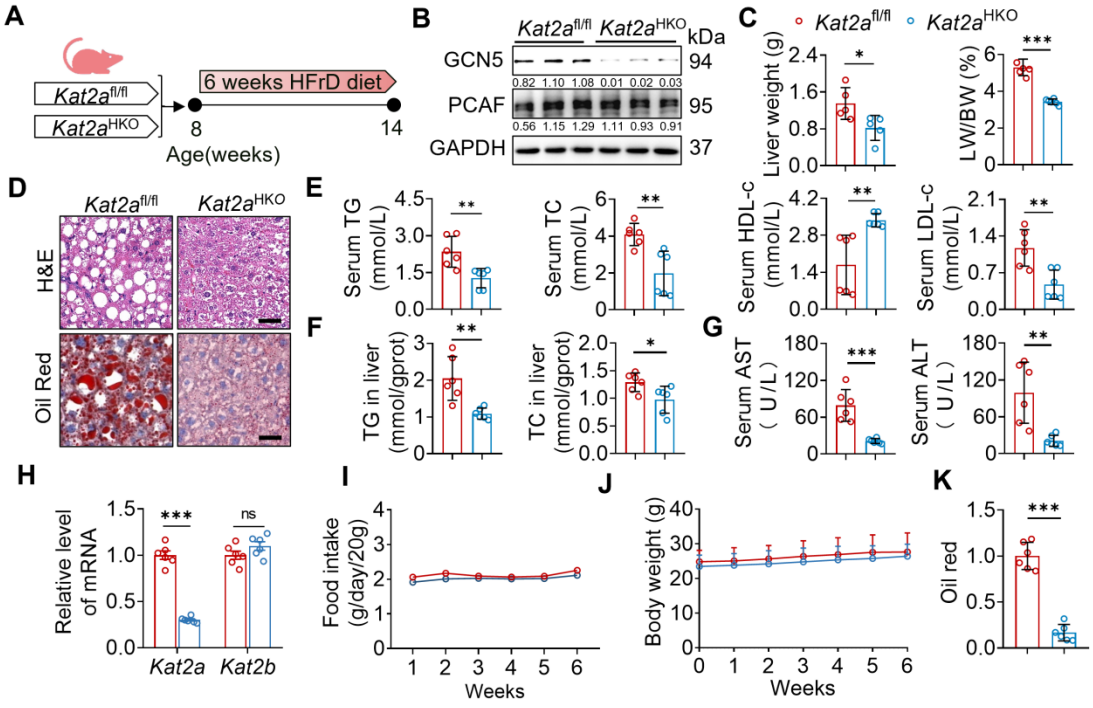
A
Kat2a fl/fl
Kat2a HKO
6 weeks HFrD diet
8
14
Age(weeks)
B
Kat2a fl/fl
Kat2a HKO
kDa
GCN5
94
0.82 1.10 1.08 0.01 0.02 0.03
PCAF
95
0.56 1.15 1.29 1.11 0.93 0.91
GAPDH
37
C
Kat2a fl/fl
Kat2a HKO
Liver weight (g)
LW/BW (%)
D
Kat2a fl/fl
Kat2a HKO
H&E
Oil Red
E
Serum TG (mmol/L)
Serum TC (mmol/L)
Serum HDL-c (mmol/L)
Serum LDL-c (mmol/L)
F
TG in liver (mmol/gprot)
TC in liver (mmol/gprot)
G
Serum AST (U/L)
Serum ALT (U/L)
H
Relative level of mRNA
Kat2a
Kat2b
ns
I
Food intake (g/day/20g)
Weeks
J
Body weight (g)
Weeks
K
Oil red

673 **Figure S5**

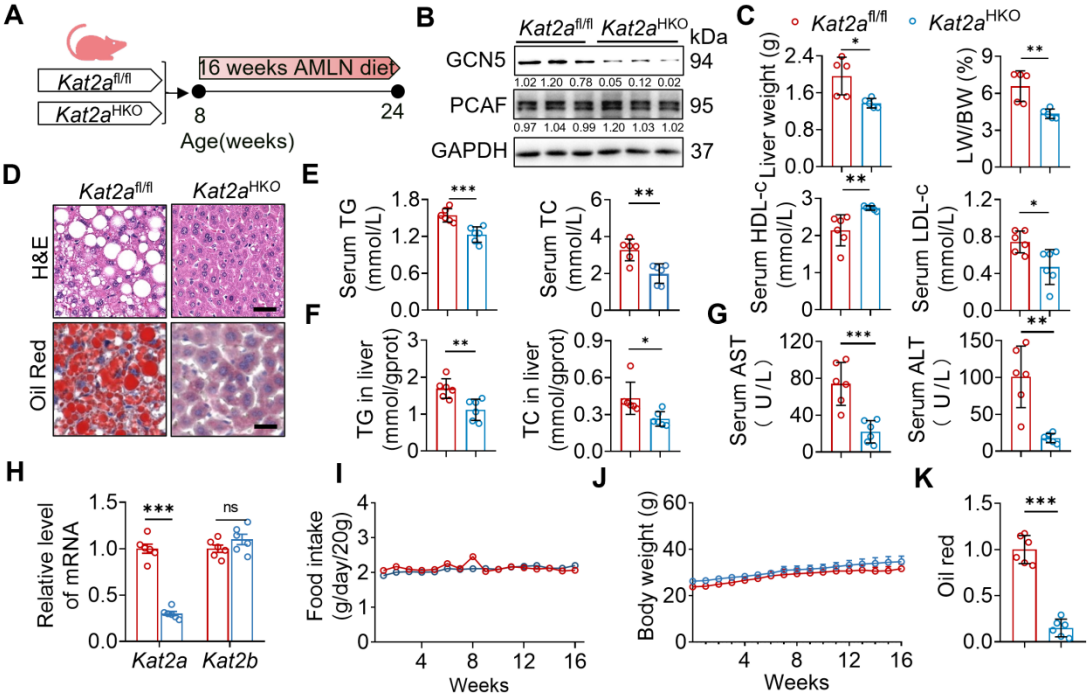

674

675

Figure S6

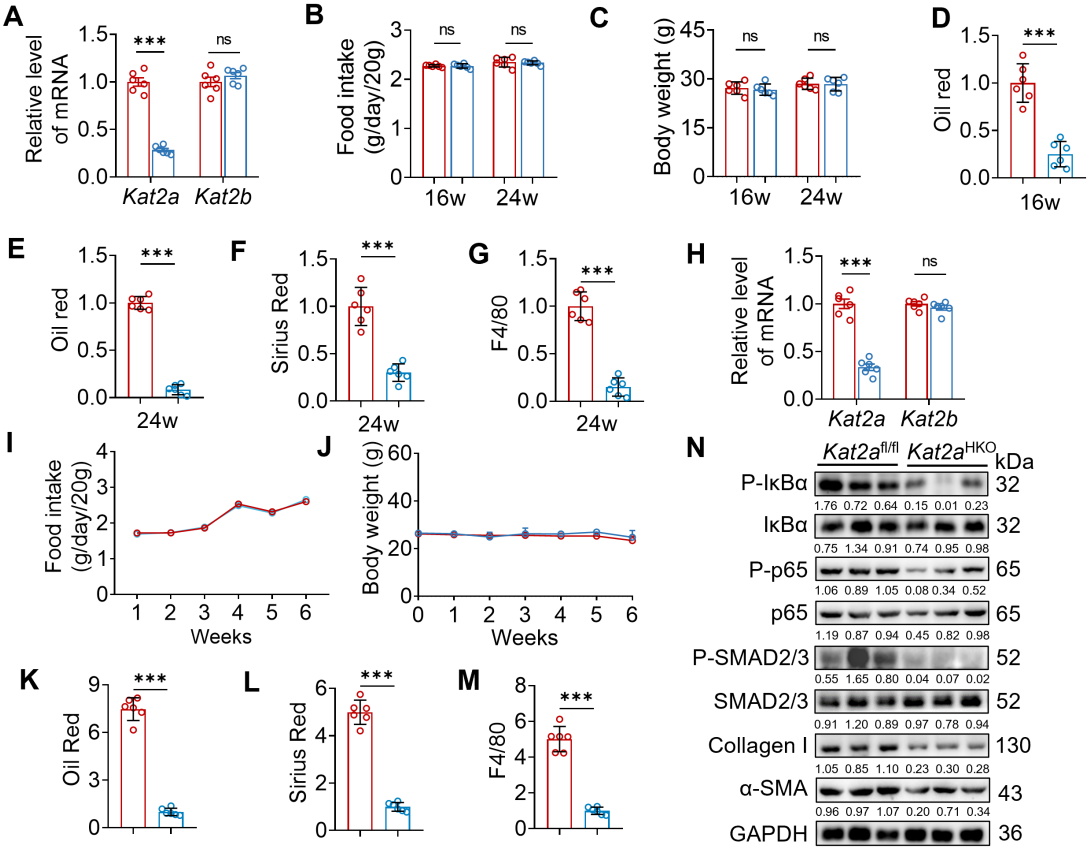
A
Relative level of mRNA
***
ns
Kat2a
Kat2b
B
Food intake (g/day/20g)
ns
ns
16w
24w
C
Body weight (g)
ns
ns
16w
24w
D
Oil red
***
16w
E
Oil red
***
24w
F
Sirius Red
***
24w
G
F4/80
***
24w
H
Relative level of mRNA
***
ns
Kat2a
Kat2b
I
Food intake (g/day/20g)
Weeks
J
Body weight (g)
Weeks
K
Oil Red
***
L
Sirius Red
***
M
F4/80
***
N
Kat2afl/fl
Kat2aHKO
kDa
P-IκBα
32
1.76 0.72 0.64 0.15 0.01 0.23
IκBα
32
0.75 1.34 0.91 0.74 0.95 0.98
P-p65
65
1.06 0.89 1.05 0.08 0.34 0.52
p65
65
1.19 0.87 0.94 0.45 0.82 0.98
P-SMAD2/3
52
0.55 1.65 0.80 0.04 0.07 0.02
SMAD2/3
52
0.91 1.20 0.89 0.97 0.78 0.94
Collagen I
130
1.05 0.85 1.10 0.23 0.30 0.28
α-SMA
43
0.96 0.97 1.07 0.20 0.71 0.34
GAPDH
36

Figure S7

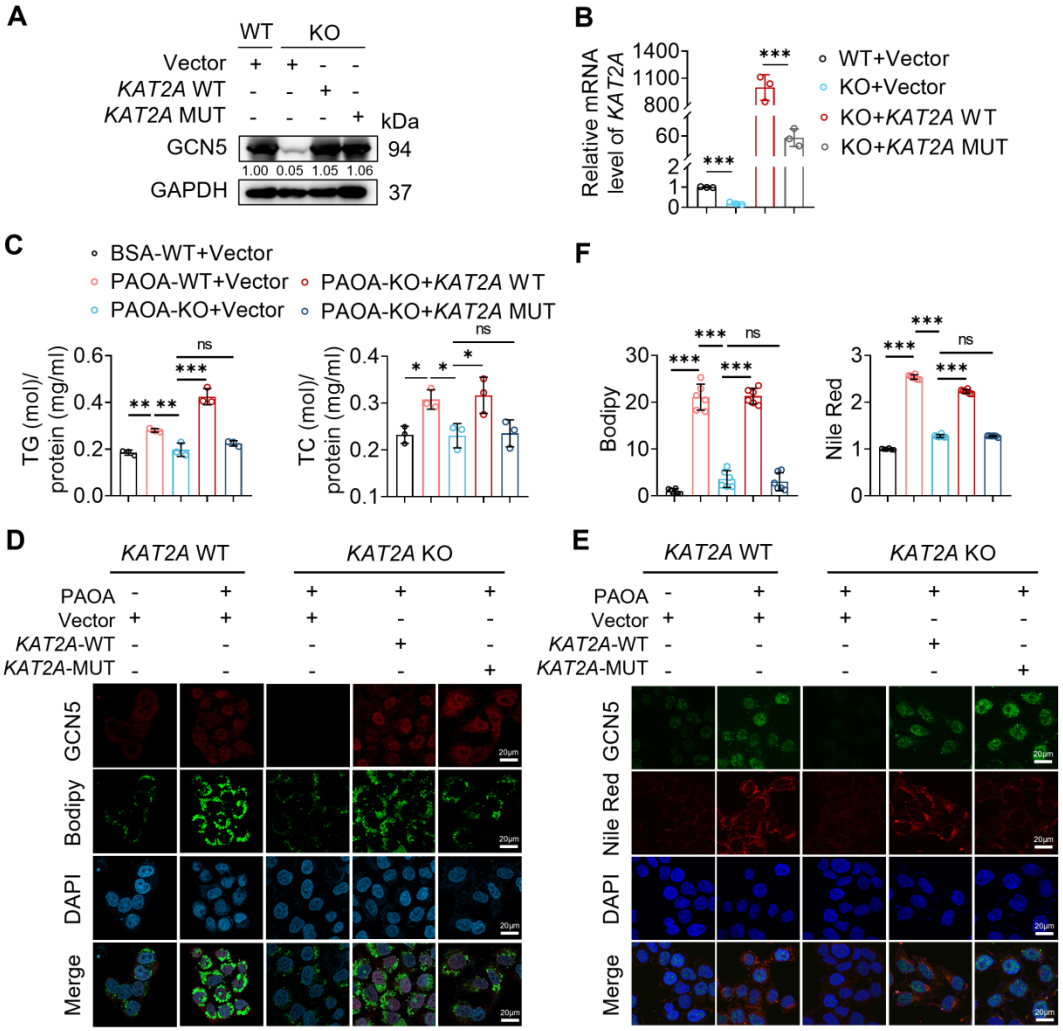
A
WT
KO
Vector
KAT2A WT
KAT2A MUT
kDa
GCN5
94
1.00 0.05 1.05 1.06
GAPDH
37
B
Relative mRNA level of KAT2A
WT+Vector
KO+Vector
KO+KAT2A WT
KO+KAT2A MUT
C
BSA-WT+Vector
PAOA-WT+Vector
PAOA-KO+Vector
PAOA-KO+KAT2A WT
PAOA-KO+KAT2A MUT
TG (mol)/ protein (mg/ml)
TC (mol)/ protein (mg/ml)
F
Bodipy
Nile Red
D
KAT2A WT
KAT2A KO
PAOA
Vector
KAT2A-WT
KAT2A-MUT
GCN5
Bodipy
DAPI
Merge
E
KAT2A WT
KAT2A KO
PAOA
Vector
KAT2A-WT
KAT2A-MUT
GCN5
Nile Red
DAPI
Merge

682 **Figure S8**

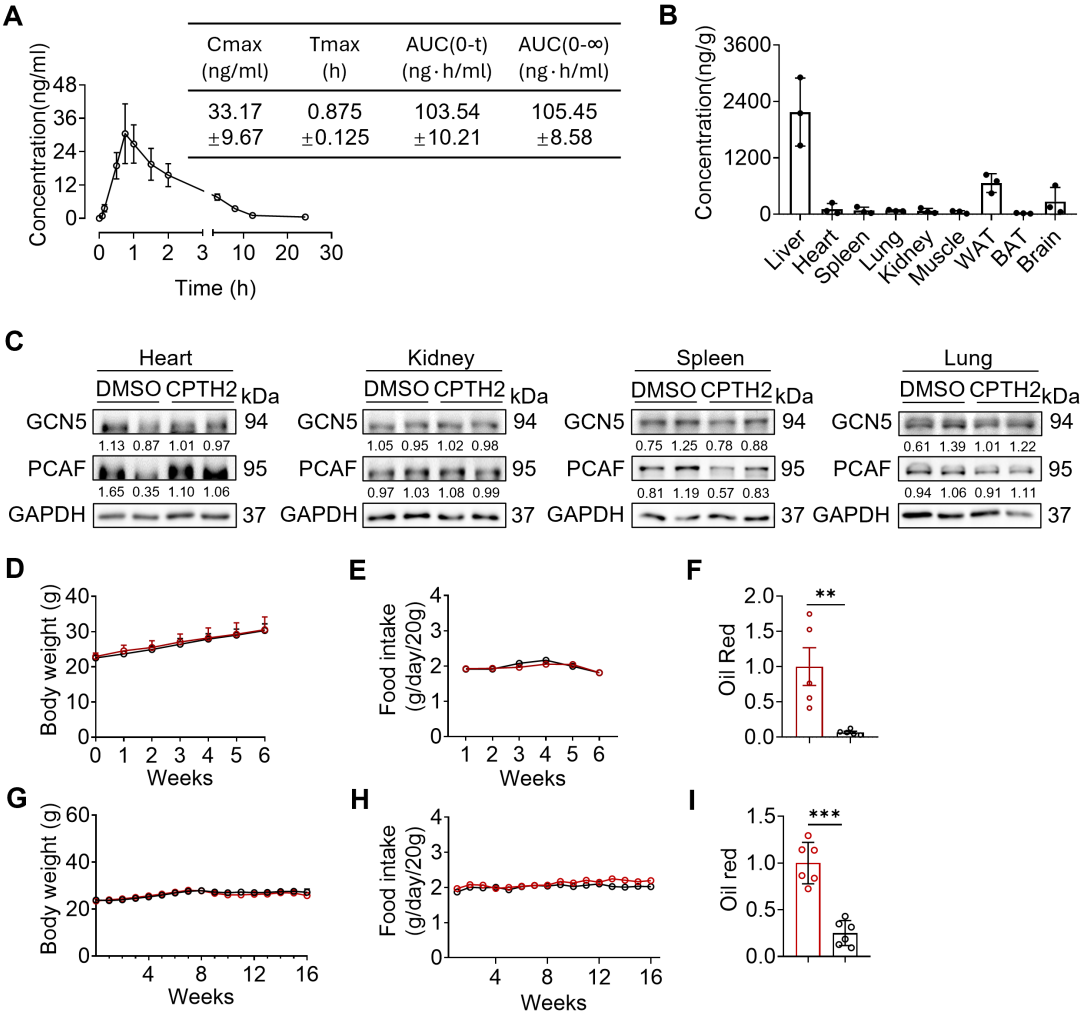

683
684

Figure S9

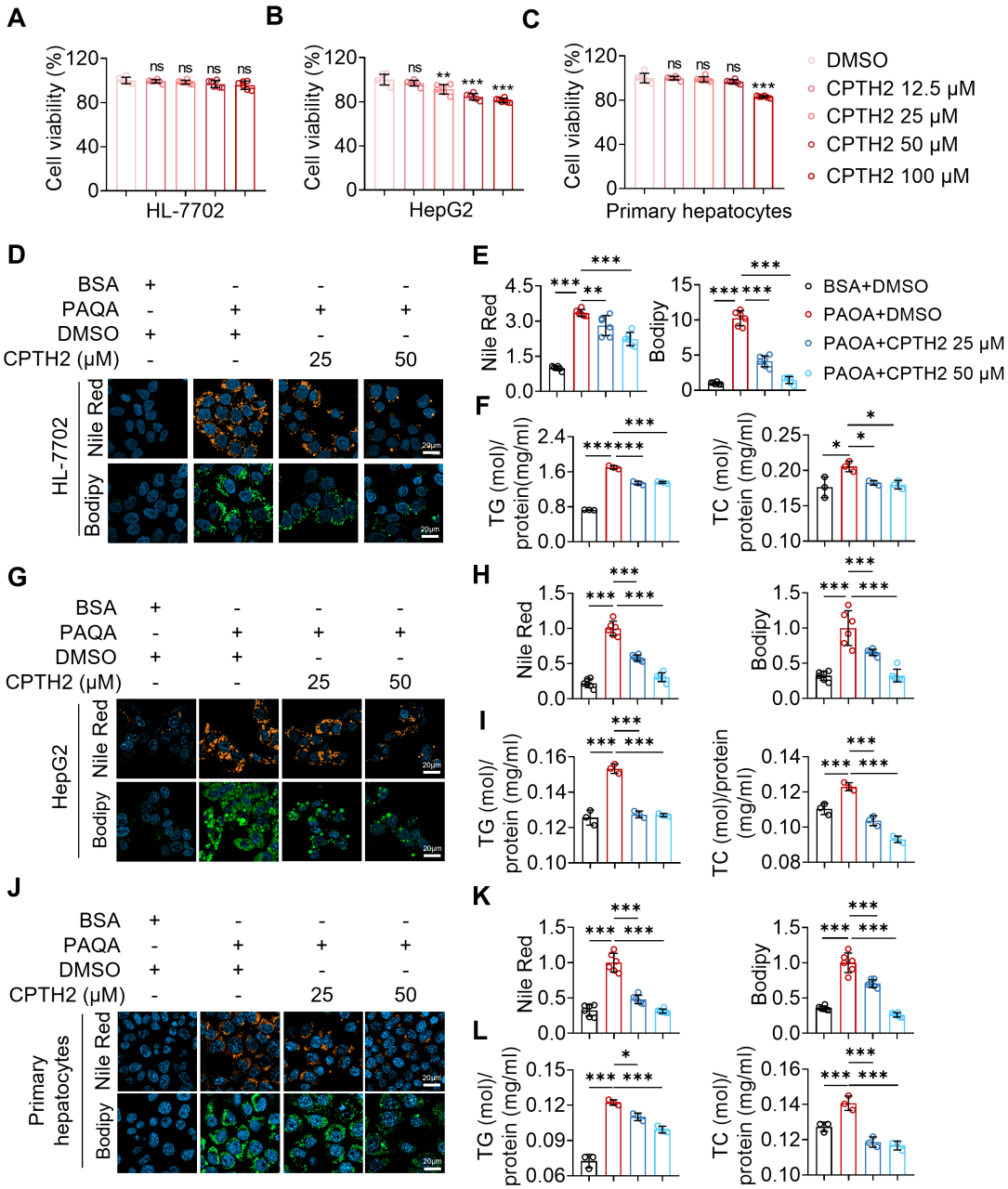
A
B
C
Cell viability (%)
HL-7702
HepG2
Primary hepatocytes
DMSO
CPTH2 12.5 μM
CPTH2 25 μM
CPTH2 50 μM
CPTH2 100 μM
D
BSA
PAQA
DMSO
CPTH2 (μM)
HL-7702
Nile Red
Bodipy
E
Nile Red
Bodipy
BSA+DMSO
PAOA+DMSO
PAOA+CPTH2 25 μM
PAOA+CPTH2 50 μM
F
TG (mol)/ protein(mg/ml)
TC (mol)/ protein (mg/ml)
G
HepG2
H
I
TG (mol)/ protein (mg/ml)
TC (mol)/protein (mg/ml)
J
Primary hepatocytes
K
L

688 **Figure S10**

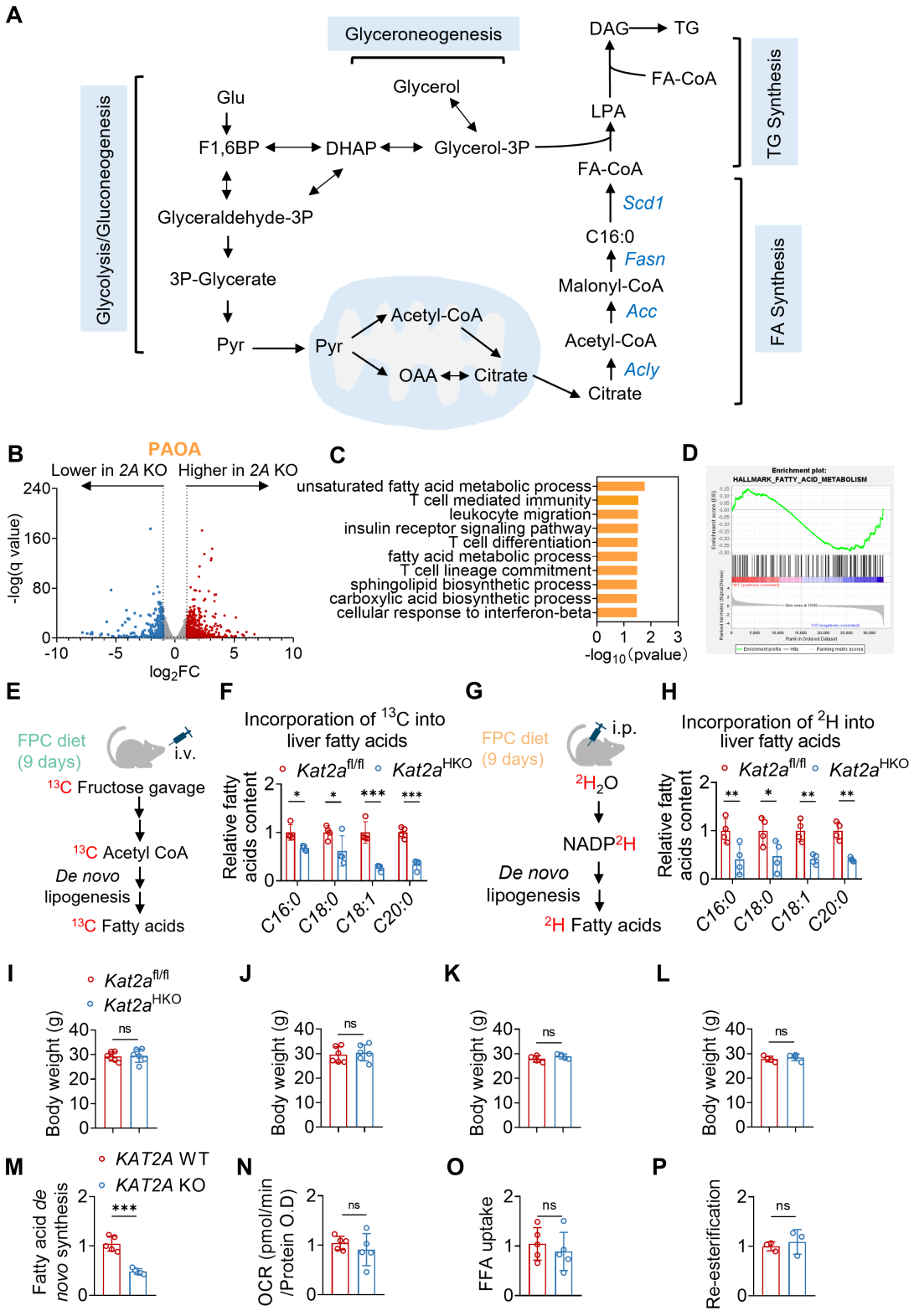

689

690

Figure S11

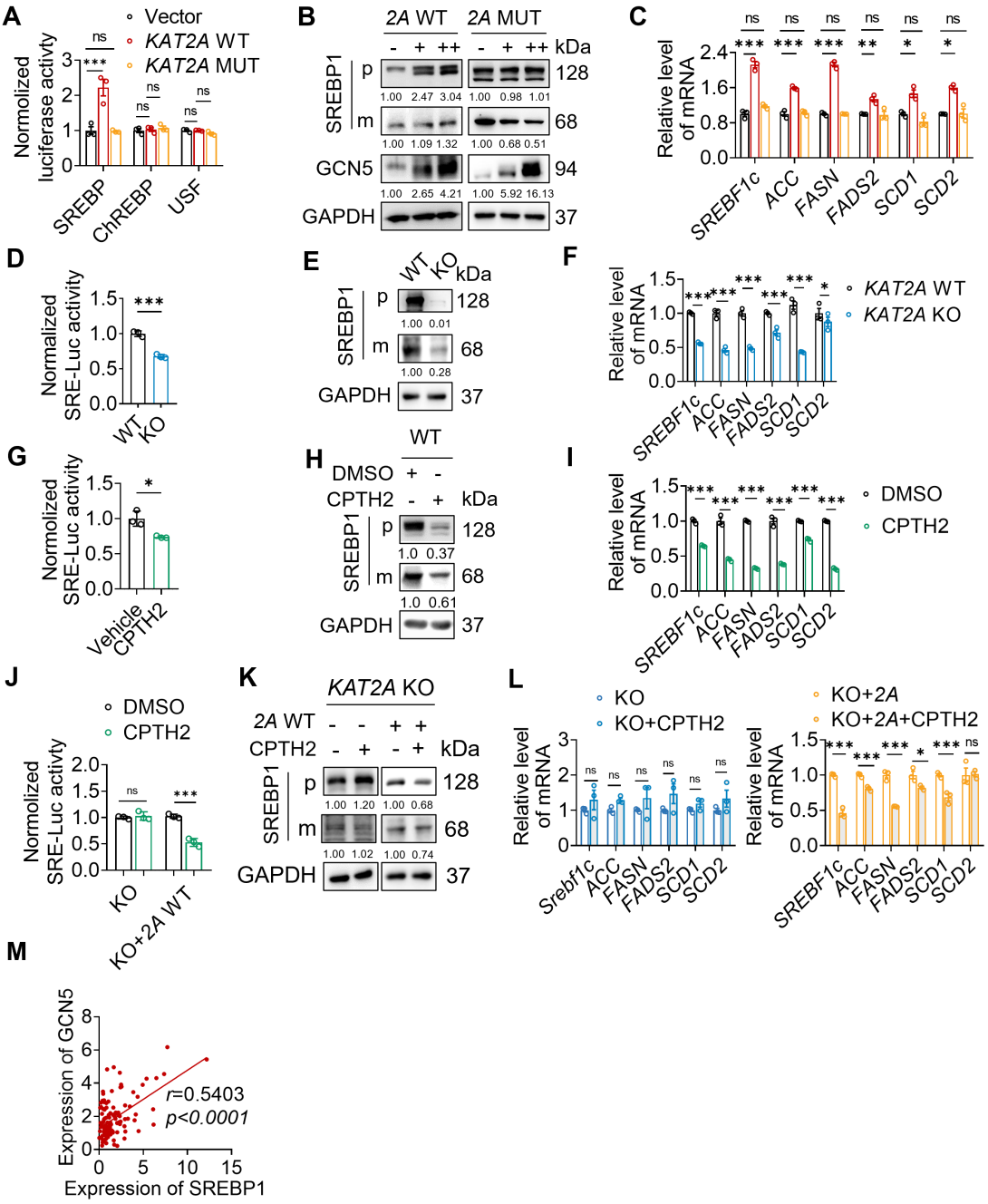
A
Vector
KAT2A WT
KAT2A MUT
Normolized luciferase activty
SREBP
ChREBP
USF
B
2A WT
2A MUT
kDa
SREBP1
p
m
GCN5
GAPDH
C
Relative level of mRNA
SREBF1c
ACC
FASN
FADS2
SCD1
SCD2
D
Normalized SRE-Luc activity
WT
KO
E
F
KAT2A WT
KAT2A KO
G
Vehicle
CPTH2
H
DMSO
CPTH2
I
J
KO
KO+2A WT
K
KAT2A KO
2A WT
L
KO
KO+CPTH2
KO+2A
KO+2A+CPTH2
Srebf1c
M
Expression of GCN5
Expression of SREBP1
r=0.5403
p<0.0001

Figure S12

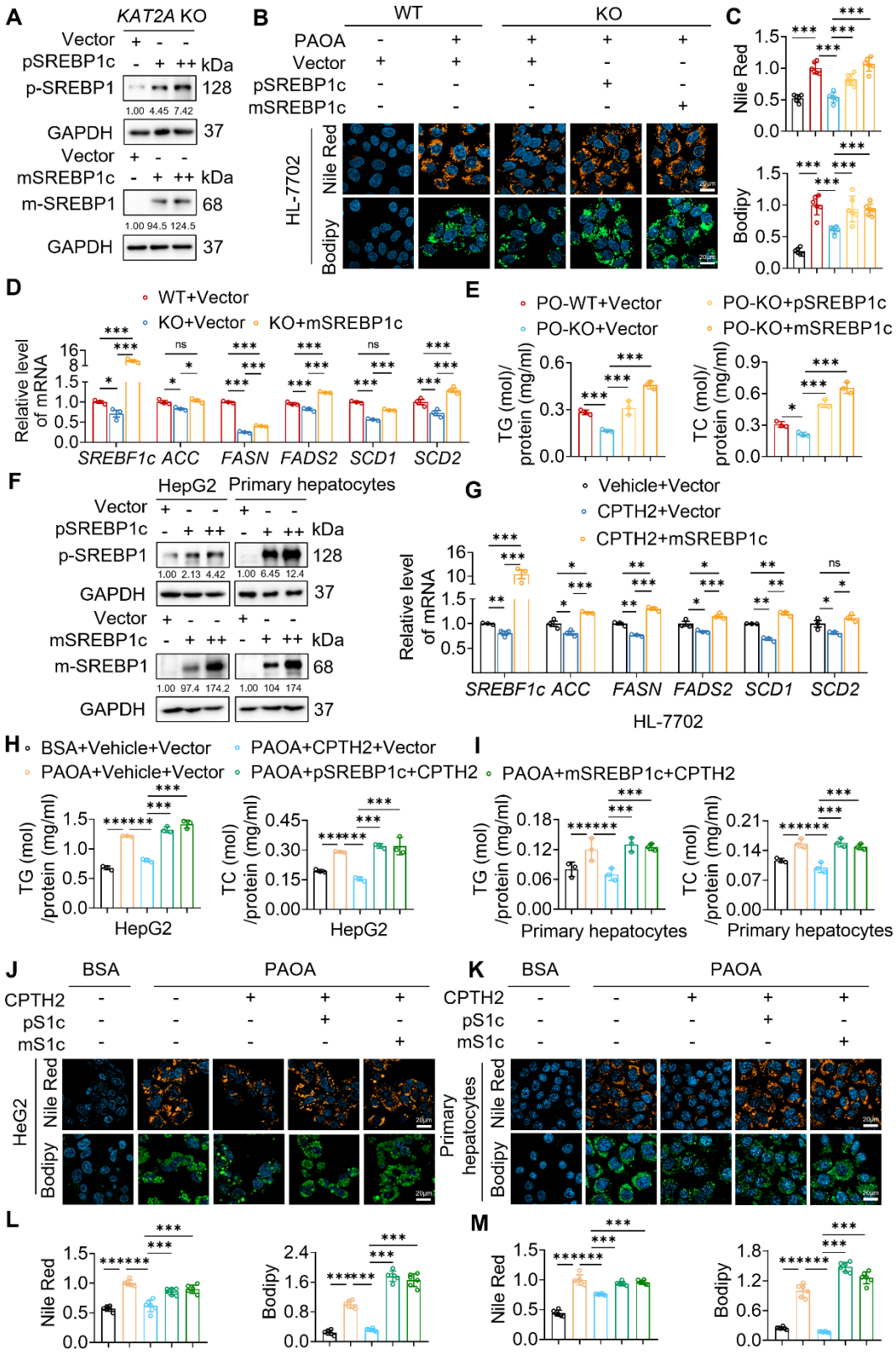
A
KAT2A KO
Vector
pSREBP1c
p-SREBP1
GAPDH
mSREBP1c
m-SREBP1
kDa
B
WT
KO
PAOA
Vector
pSREBP1c
mSREBP1c
HL-7702
Nile Red
Bodipy
C
Nile Red
Bodipy
D
WT+Vector
KO+Vector
KO+mSREBP1c
Relative level of mRNA
SREBF1c ACC FASN FADS2 SCD1 SCD2
E
PO-WT+Vector
PO-KO+Vector
PO-KO+pSREBP1c
PO-KO+mSREBP1c
TG (mol)/ protein (mg/ml)
TC (mol)/ protein (mg/ml)
F
HepG2
Primary hepatocytes
G
Vehicle+Vector
CPTH2+Vector
CPTH2+mSREBP1c
HL-7702
H
BSA+Vehicle+Vector
PAOA+Vehicle+Vector
PAOA+CPTH2+Vector
PAOA+pSREBP1c+CPTH2
TG (mol) /protein (mg/ml)
TC (mol) /protein (mg/ml)
HepG2
I
PAOA+mSREBP1c+CPTH2
Primary hepatocytes
J
BSA
PAOA
CPTH2
pS1c
mS1c
HeG2
K
Primary hepatocytes
L
M

Figure S13

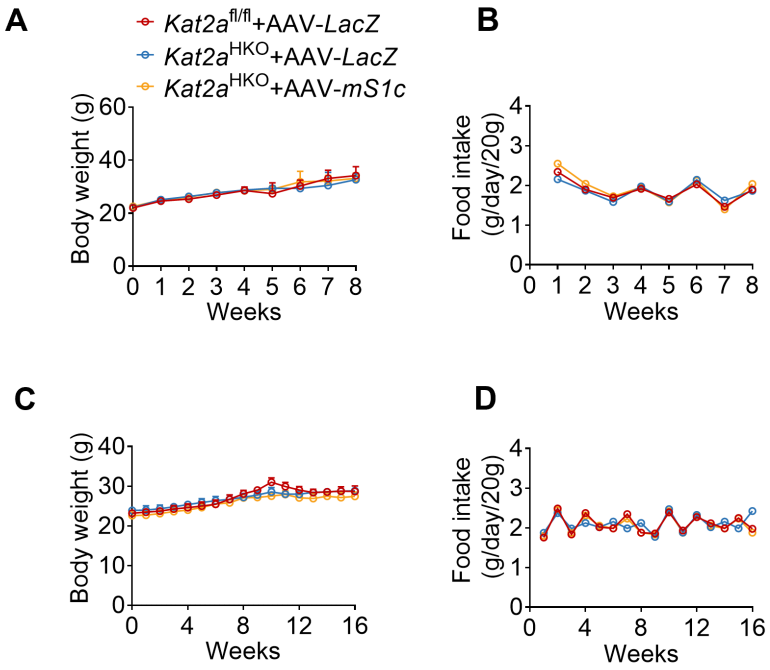
A
Kat2a^fl/fl+AAV-LacZ
Kat2a^HKO+AAV-LacZ
Kat2a^HKO+AAV-mS1c
Body weight (g)
Weeks
B
Food intake (g/day/20g)
Weeks
C
Body weight (g)
Weeks
D
Food intake (g/day/20g)
Weeks

Figure S14

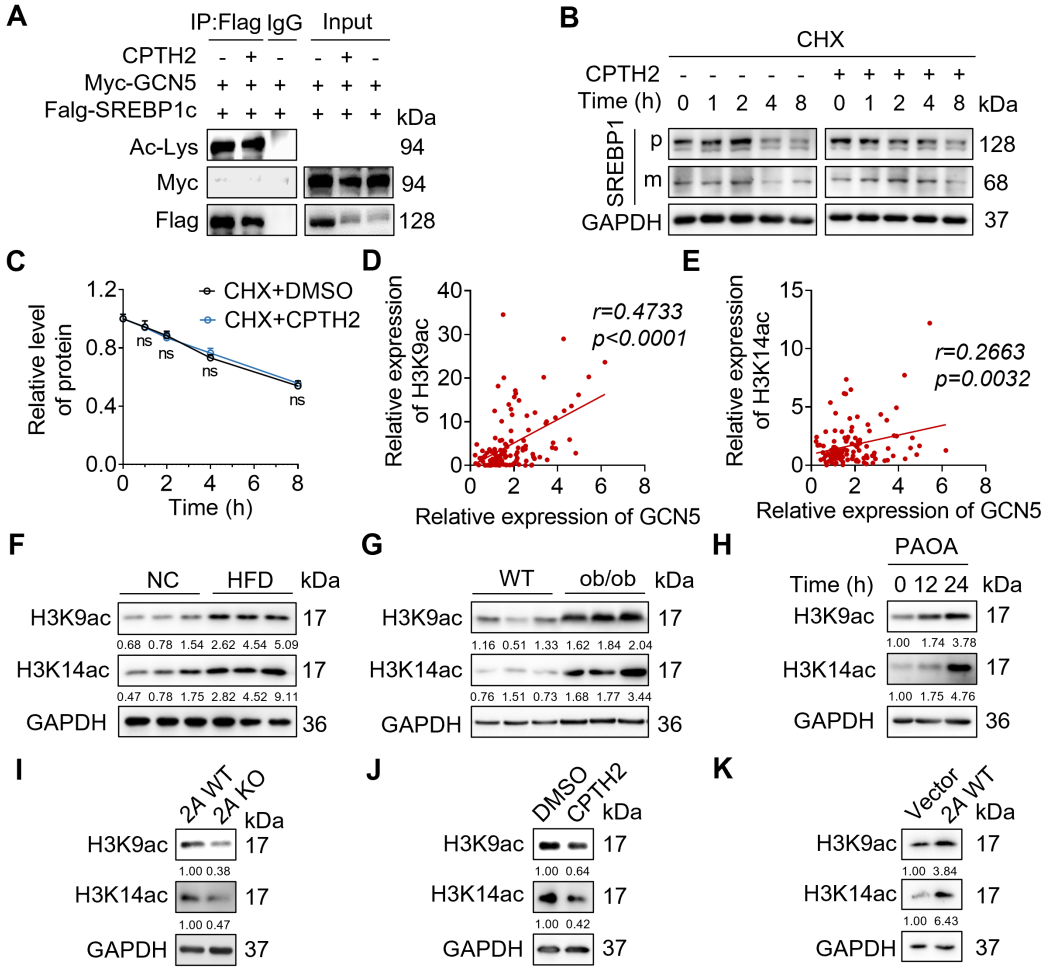
A
IP:Flag IgG
Input
CPTH2
Myc-GCN5
Falg-SREBP1c
kDa
Ac-Lys
Myc
Flag
94
94
128
B
CHX
CPTH2
Time (h) 0 1 2 4 8 0 1 2 4 8 kDa
SREBP1
p
m
GAPDH
128
68
37
C
CHX+DMSO
CHX+CPTH2
Relative level of protein
Time (h)
ns
D
Relative expression of H3K9ac
Relative expression of GCN5
r=0.4733
p<0.0001
E
Relative expression of H3K14ac
Relative expression of GCN5
r=0.2663
p=0.0032
F
NC
HFD
kDa
H3K9ac
H3K14ac
GAPDH
17
17
36
0.68 0.78 1.54 2.62 4.54 5.09
0.47 0.78 1.75 2.82 4.52 9.11
G
WT
ob/ob
kDa
H3K9ac
H3K14ac
GAPDH
17
17
36
1.16 0.51 1.33 1.62 1.84 2.04
0.76 1.51 0.73 1.68 1.77 3.44
H
PAOA
Time (h) 0 12 24 kDa
H3K9ac
H3K14ac
GAPDH
17
17
36
1.00 1.74 3.78
1.00 1.75 4.76
I
2A WT
2A KO
kDa
H3K9ac
H3K14ac
GAPDH
17
17
37
1.00 0.38
1.00 0.47
J
DMSO
CPTH2
kDa
H3K9ac
H3K14ac
GAPDH
17
17
37
1.00 0.64
1.00 0.42
K
Vector
2A WT
kDa
H3K9ac
H3K14ac
GAPDH
17
17
37
1.00 3.84
1.00 6.43

Figure S15

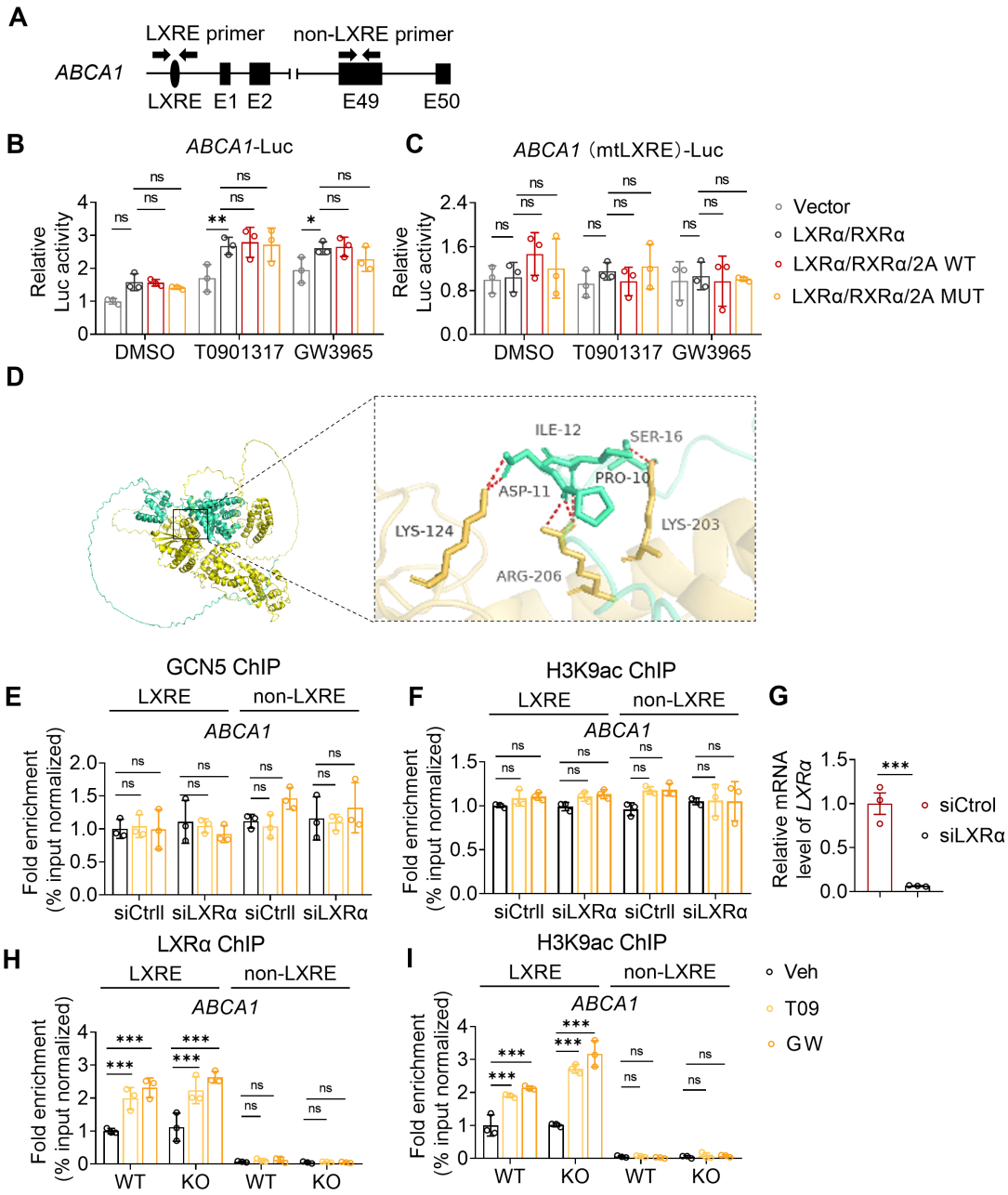
A
LXRE primer
non-LXRE primer
ABCA1
LXRE E1 E2
E49 E50
B
ABCA1-Luc
Relative Luc activity
DMSO T0901317 GW3965
C
ABCA1 (mtLXRE)-Luc
Relative Luc activity
DMSO T0901317 GW3965
Vector
LXRα/RXRα
LXRα/RXRα/2A WT
LXRα/RXRα/2A MUT
D
ILE-12
SER-16
PRO-10
ASP-11
LYS-124
LYS-203
ARG-206
E
GCN5 ChIP
LXRE non-LXRE
ABCA1
Fold enrichment (% input normalized)
siCtrll siLXRα siCtrll siLXRα
F
H3K9ac ChIP
LXRE non-LXRE
ABCA1
Fold enrichment (% input normalized)
siCtrll siLXRα siCtrll siLXRα
G
Relative mRNA level of LXRα
siCtrol
siLXRα
H
LXRα ChIP
LXRE non-LXRE
ABCA1
Fold enrichment (% input normalized)
WT KO WT KO
I
H3K9ac ChIP
LXRE non-LXRE
ABCA1
Fold enrichment (% input normalized)
WT KO WT KO
Veh
T09
GW

Figure S16

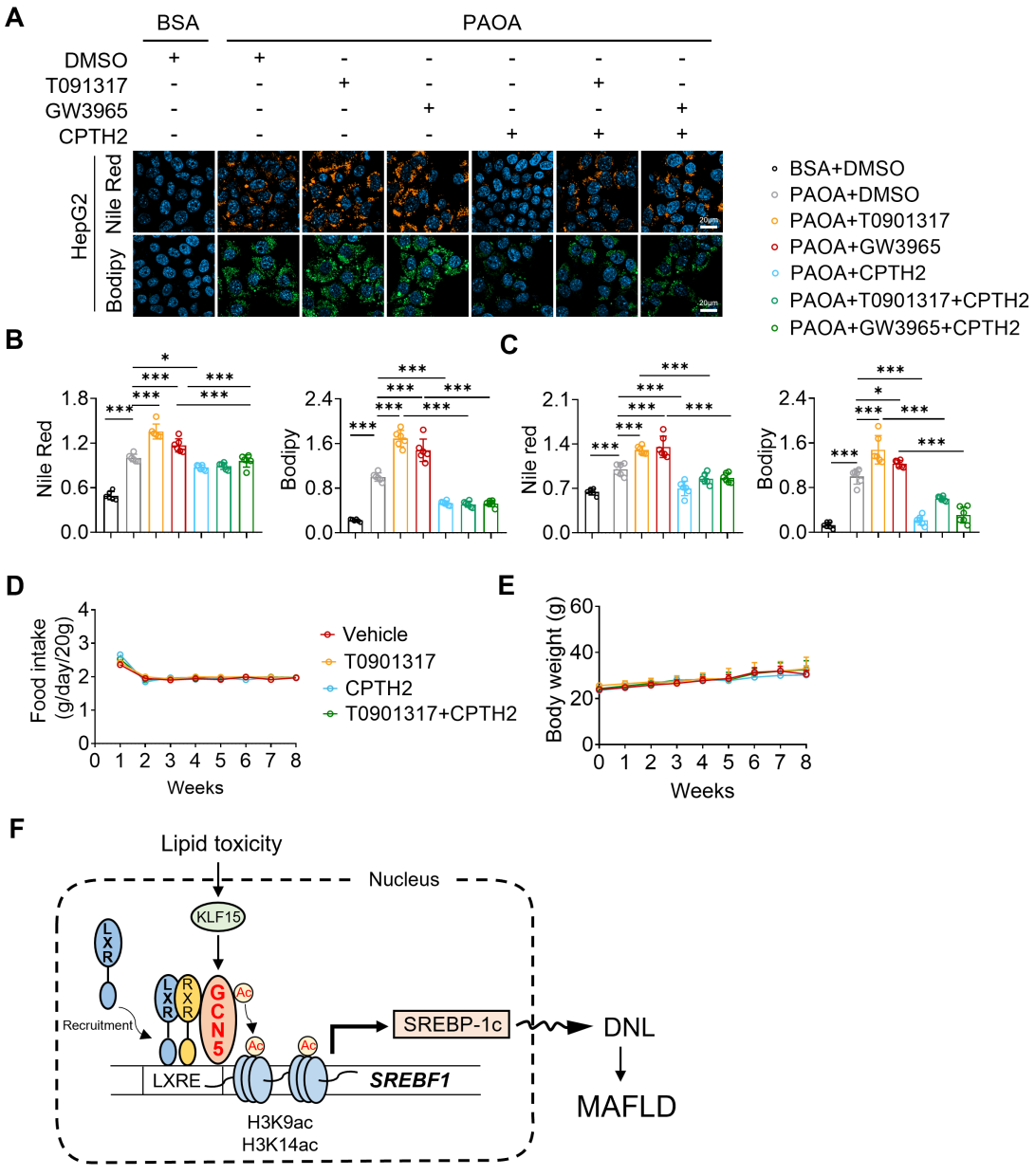
A
BSA
PAOA
DMSO
T091317
GW3965
CPTH2
HepG2
Nile Red
Bodipy
BSA+DMSO
PAOA+DMSO
PAOA+T0901317
PAOA+GW3965
PAOA+CPTH2
PAOA+T0901317+CPTH2
PAOA+GW3965+CPTH2
B
Nile Red
Bodipy
C
Nile red
Bodipy
D
Food intake (g/day/20g)
Weeks
Vehicle
T0901317
CPTH2
T0901317+CPTH2
E
Body weight (g)
Weeks
F
Lipid toxicity
Nucleus
KLF15
LXR
RXR
GCN5
Ac
Recruitment
LXRE
SREBF1
SREBP-1c
DNL
MAFLD
H3K9ac
H3K14ac